WOLKITE UNIVERSITY

NATURAL AND COMPUTITIONAL SCIENCE

CHEMICAL DEPOSITION OF POLYANILINE ON THE SURFACE OF MORINGA OLIFERA SEED FOR WASTEWATER TREATMENT

M.Sc. Thesis By

AYANSA FIKADU G/MARIAM

June 19, 2023

Wolkite University

Chemical Deposition of Polyaniline on the Surface of Moringa Olifera for Wastewater Treatment

This thesis Submitted to School of Graduate studies

Wolkite University

In partial fulfillment of the requirements of the Degree of Master of Science in Chemistry (Analytical)

BY

AYANSA FIKADU G/MARIAM

June 19, 2023

Wolkite University

Approval Sheet

Wolkite University

School of Graduate Studies

We here by certify that we have read and evaluated this thesis entitled "Chemical Deposition of Polyaniline on the Surface of Moringa Olifera Seed for Wastewater Treatment" prepared under my guidance. We recommended that it be submitted as fulfilling the thesis requirement.

……	…….	……...
Name of Major Advisor	Signature	Date
……	…….	……...
Name of Co-advisor	Signature	Date

As a member of the board of examiners of MSc thesis open defense examination, We certify that we have read and evaluated the Thesis prepared by Ayansa Fikadu G/Mariam and examined the candidate. We recommended that the Thesis be accepted as fulfilling the thesis requirements for the degree of Master of Science in Chemistry (Analytical).

……	…….	……...
Name of Chairman	Signature	Date
……	……	……...
Name of Internal Examiner	Signature	Date
……	…….	……...
Name of External Examiner	Signature	Date

Acknowledgement

I am heartily thankful to my supervisors Dr. Alula Yohanis and Dr. Israel Leka who are willing to support and work with me. Their comments and feedbacks are constructive and valuable for successful completion of the work with such a limited resource and many more challenges. I sincerely acknowledge and especially thankful for Dr. Israel Leka of chemistry department head for his unreserved support in language editing and laboratory analysis. I offer my regards and blessings to all my friends who supported me in any circumstance during planning, experiment and analysis of the project. Lastly, I want to express my deepest and warmest gratitude to my family. My wife, it is all your support and at this stage I want to acknowledge your effort and I am proud of you. The way you handle family matters, and nurturing our kids is always appreciable. My kids, your love are a motive for my success. I feel enormously blessed having you at every step of my life

Contents

List of Table **Page**

LIST OF FIGURES

Figure **Page**

LIST OF ABBREVIATIONS

XRD	X-ray Diffraction
FTIR	Fourier Transforms Infrared Spectroscopy
SEM	Scanning Electron Microscopy
PANI	Polyaniline
MO	Moringa Olifera
PANI/MO	Polyaniline coated on Moringa Olifera
PANI/SiO_2	Polyaniline coated on silica
PANI/Fe_2O_4	Polyaniline coated on Iron Oxide
PANI/GO	Polyaniline coated on Graphene Oxide
WHO	World Health Organization
EPA	Environmental Protection Agency
USA	United State of America
MOS	Moringa olifera seed
ZnO-NP	Zinc oxide nanoparticle
MgO-NP	Magnesium oxide nanoparticle
NiO-NP	Nickel oxide nanoparticle
G	GUBRE
WES	Worket Elementary School
MT	Middle Torhegne
THC	Torhegne Health Center

ABSTRACT

Water technology advancement coupled with environmental concern, increasing water demand, and the living standards of society led to the technology that provides clear water to the ecosystem. This study was give best alternative that surface modification of PANI on MO in which low-cost, effective, and environmentally friendly adsorbents new and innovated for water treatment technology. Thus, PANI/MO was synthesized by in situ oxidative polymerization of aniline on moringa olifera seed for wastewater treatment applications and study the physico-chemical parameter of wastewater generated from Enamor Woreda, Gurage Zone, SNNPR, Ethiopia. The values of most of the physicochemical parameters, and heavy metals were above the acceptable range for wastewater discharge limits set by WHO. The correlation coefficient of physico-chemical parameter between the four wastewater sampler was strong, and moderate correlation between all parameter(TDS,EC,TSS, pH, TA, and TH), while weak correlation between turbidity TDS, EC, TSS, pH, TA, TH, and Temp. The prepared nano-composites were characterized by powder XRD, FT-IR, UV spectroscopy and conductimeter. SEM and XRD studies reveal that the crystal structures of embedded MO were amorphous with semi-crystalline, while PANI, PANI/MO nanoparticles distorted and become porous with polycrystalline. Vibrational spectra analysis confirms that adsorbed PANI nanoparticles on the surface of MO acts as a compensator for positively PANI nanoparticles in the formation of PANI/MO nano composites. UV-visible spectroscopy showed that PANI/MO has a smaller band gap compared with MO; this implies that PANI/MO has a higher probability of absorbing light, being optically active, or being chemically reactive. The experiment found that the PANI/MO composites had a best adsorption capacity for copper (10.01 mg/g) and lead (23.01 mg/g) in simulated wastewater solutions. When all parameters were optimized (pH at 5, contact time at 30 minutes, temperature at 25^0c, and 2 gram of PANI/MO) removal adsorption efficiency for Pb^{2+} (99%), and Cu^{2+} ions(97.77%). *The Freundlich isotherm data for Cu^{2+} and Pb^{2+} have a good fit with the experimental data (R^2 = 0.99 and 0.98), respectively. Cu^{2+} and Pb^{2+} Langmuir isotherm data (R_L=0.18 & 0.19). The pseudo second order kinetic isothermal was more fit with physic-sorption at (R^2=0.99 for Cu^{2+} and R^2=1 for Pb^{2+}). The PANI/MO composite shows antibacterial activity against the bacterial species.*

Keyword:- Polyaniline, moringa Olifera, PANI/MO composite, Copper (II), Lead (II)

CHAPTER ONE: INTRODUCTION

1.1 Background

Water technology advancement coupled with environmental concern, increasing water demand, and the living standards of society led to the technology that provides clear water to the ecosystem. Heavy metals have been considered one of the major contaminants of water in recent years due to their non-biodegradable properties, making them toxic and bio-accumulating in living organisms [1].

Many methods have used for the removal of heavy metal ions from wastewater, including chemical precipitation, chemical oxidation and reduction, ion exchange, filtration, membrane technologies, ozonation, coagulation and flocculation, electrochemical treatment, and evaporative recovery. However, these high-technology processes have significant limitation, including incomplete metal removal, requirements for expensive equipment and monitoring systems, high costs and reagents, energy requirements, and the generation of toxic sludge or other waste products that require disposal. Consequently, it remains challenging to develop an efficient, economical, and sustainable technology [2]. In the past two decades, the adsorption of heavy metals with environmentally friendly and economical materials like agricultural, industrial, or urban residues has emerged as a promising technology for the removal of pollutants from wastewater treatment. Hence, many authors using economical adsorbents such as lignin, bark, chitosan, clay, zeolite, activated carbons, and synthetic polymeric adsorbents reported a lot of research [2].

Adsorption onto activated carbon was one method for removing toxic metal ions, but the high cost of activated carbon restricts its use in Ethiopia. The adsorption abilities of a number of low-cost adsorbents have been determined for the removal of heavy metals from water. In addition to the exhaustion of coal, the price of active carbon increased, so without affecting this factor, we have used activated carbon composite, and most importantly, activated carbon composite could be effective absorbents for heavy metal contaminants. Due to the expensive source of activated carbon adsorbent, carbonaceous material was converting into activated carbon for heavy metal removal [3].

In 1991, Iijima discovered that CNT (carbon nanotube) gives the best results for eliminating toxic metal ions like cadmium, copper, lead, chromium, and nickel from groundwater. The

carbon nanotube adsorption gives excellent results in the removal of these heavy metals. In 2010, a researcher Jiang examined the kaolinite-clay, which has used for the elimination of toxic heavy metals from wastewater contamination. The time was approximately 29–30 minutes. In 2009, the two researchers Navia and Agoubordea investigated that sediments and sawdust, and sometimes a mix of both materials, were used as adsorbents for the elimination of Pb^{2+} and Cu^{2+} from wastewater, but they also had lower removal efficiency from wastewater contaminates. However, the procedures of carbon nanotube adsorbents are very complex in nature, so the mechanism was through chemical interaction, electrostatic attraction, and sorption precipitation in-between the surface of the functional group and the heavy metal ions of the carbon nanotube adsorbents [4].

In 2011, Fu and Wang discovered the most efficient techniques for removing heavy metal ions that synthesized. Gopalakrishnan et al. (2015) describe the quality of nano-materials that possess the functional group, have a high surface area, and enhance the active site. Due to these qualities, heavy and unwanted metal ion was removing easily. Renu et al. (2017) describe adsorption techniques for the removal of toxic metal ions with the use of commercial adsorbent and bio-adsorbent, which increase the removing capacity [3, 5].

Sabry M. Shaheen et al. discover that with the help of zeolite in adsorption techniques, the elimination of heavy metal ions will take place with better efficiency. K. Singh et al. found that adsorbents like composites of carbon nanotubes, alumina, graphite sand composites, eggshell, and many more has used to eliminate toxic metal ions like copper and lead from the groundwater effluent [4]. However, the proposed materials are costly and scarce, which makes their work less interesting, and the search for highly active and simple materials remains a challenge. Therefore, a cheap, available, and highly active material has needed to solve the aforementioned problems [2, 5].

Ethiopia is a developing country with a poor economic situation that requires low-cost drinking water treatment solutions for the affected communities that require conventional or advanced drinking water treatment. Application of plant materials for drinking water treatment is environmentally sustainable and cost-effective as they are locally available, non-toxic, easy to prepare, and the residuals generated are easy to dispose of [5].

The MO plant has received much attention within the scientific community due to its impressive medicinal properties and environmental applications. This plant is native to Ethiopia and is

nowadays cultivated in many parts of the world since it grows in arid, tropical, and semi-tropical areas. The different parts of MO, including leaves, seeds, flowers, and fruits, contain a great variety of chemical compounds responsible for this species' properties [6].

In their research, Aisida et al. synthesized a green and environmentally friendly approach for nanoparticles by using an aqueous extract of the Moringa olifera plant as a reluctant and capping agent. Elumalai et al. employed a straightforward and environmentally safe chemical route to synthesized zinc oxide nanoparticles (ZnO-NPs) from Moringa olifera leaf extract. Antimicrobial activity studies confirmed the presence of maximum inhibition [7].

Ezhilarasi et al. synthesized the nickel oxide nanoparticles (NiO-NPs) using the green method. Fatiqin et al. was synthesized magnesium oxide nanoparticles (MgO-NPs) in this work by combining Moringa olifera seed extracts with a magnesium chloride solution. It shows cytotoxicity and antibacterial activity [4, 8].

Ravi Kumar and Sheeja (2013) conducted the analysis of the heavy metals cadmium, copper, chromium, and lead before and after treatment of water with MO seed biopolymer. The results showed that the percentage removal by Moringa olifera seed was 95% for copper, 93% for lead, 76% for cadmium, and 70% for chromium. However, the removal of copper and lead after coagulation with Moringa olifera seed coagulant was not as per the limits of pure groundwater standards. Therefore, additional treatments have needed to achieve the WHO standard [8]. Due to this problem, surface modification of Moringa olifera using conducting polymers such as PANI, polypyrrole, and polypheneylene is an attractive approach that has received the attention of researchers due to its flexibility, lightweight, conductivity, corrosion resistance, environmental stability, and high active surface area [10].

PANI was the most desirable due to the monomer's low cost, chemical and environmental stability, ease of synthesis, high electrical conductivity, and biocompatibility; furthermore, it possesses a large number of amine and imine functional groups that interact with some metal ions due to the strong affinity of nitrogen atoms. For this reason, polyaniline has been chosen as a platform to build innovative nano-composite adsorbents by mixing it with other moringa olifera that exhibit better adsorption capacities, chemical and thermal stability, good regeneration ability, and selectivity towards heavy metals using simple synthesis methods. The conducting polymers (CPs) in PANI have attracted great attention for wastewater treatment owing to their

intriguing properties such as ease of synthesis, tunable structure, and the presence of ideal functional groups. Therefore, the conducting polymers PANI has been widely studied due to its low cost, ease of synthesis, good environmental stability, unique doping and de-doping properties, and relatively high conductivity [10].

In general, the appearance of new water technologies known as "clean and friendly to the environment" using renewable and green materials of the moringa olifera with polyaniline entities to provide possibly the most efficient and convincing solution to the inherent problems in ground water treatment was prepared. Despite a number of papers that have been reported, to our knowledge, no paper has been reported with a new, innovative composite of polyaniline-coated Moringa olifera seed for the effective removal of Cu^{2+} and Pb^{2+} ions from groundwater.

1.2 Statement of the Problem

Water is one of the most important natural resources needed for the lives of both animals and plants. Ideally, the water resources that has used by humankind should be pure and free from different contaminants for the safety and health of human beings. However, these water sources are vulnerable to different pollutants, such as the heavy metals Pb^{2+} and Cu^{2+}, which are toxic to humans. In Ethiopia, the main source of water supply for both urban and rural communities is underground water, which accounts for 70% of the total water supply of the nation. Health issues caused by high levels of heavy metals in drinking water are a widespread problem around the world, including in Ethiopia [11]. This complexity was because a number of the treatments described in the earlier report are expensive and may not be feasible options for poor nations. Therefore, due to this, it was crucial to develop a new, innovative water treatment technology for the removal of heavy metals from wastewater.

1.3 Significance of the Study

The significance of this research was the utilization of Moringa olifera modified adsorbent with chemical polymerization of aniline and the efficiency of this modified adsorbent for the removal of basic toxic Cu^{2+} and Pb^{2+} from wastewater for ensuring a healthy environment. Beside, this study were expect to produce a comparable polyaniline-coated moringa olifera meeting the requirements of an effective adsorbent for Cu^{2+} and Pb^{2+} in wastewater treatment. In addition, these works were base to give an alternative direction towards the treatment of polyaniline-coated Moringa olifera seed wastewater.

1.4 Scope of the Study

The scope of this study was to test wastewater for the removal of Cu^{2+} and Pb^{2+} using PANI/MO as an adsorbent. Batch studies were conduct using synthetic Cu^{2+} and Pb^{2+} solutions. The influence of pH, contact time, initial metal ion concentration, temperature, and adsorbent concentration was investigate to optimize the conditions for maximum Cu^{2+} and Pb^{2+} removal. Water quality analysis of the Cu^{2+} and Pb^{2+} were done using a UV-visible spectrophotometer (Ach DM-6000). Due to time constraints, budget constraints, and limited resources, this research only focuses on the surface modification of MO by PANI and uses it for the adsorptive removal of Cu^{2+} and Pb^{2+}.

1.5 Research Objectives

1.5.1 General Objective

- The overall aim of this research paper was chemical deposition of polyaniline on the surface of moringa olifera seed for wastewater treatment.

1.5.2 The Specific Objectives

1. To study the physico-chemical properties of wastewater collected from Torhegne Health center, Middle Torhegne, Worket Elementary school, and Gubre town, Gurage zone, Ethiopia.
2. To synthesized polyaniline-coated Moringa oliefera for adsorptive removal of Cu^{2+} and Pb^{2+} from wastewater.
3. To characterize polyaniline-coated Moringa oliefera for adsorptive removal of Cu^{2+}, and Pb^{2+} from wastewater.
4. To study the effect of adsorption parameters (e.g. pH, adsorption doses, contact time, initial concentration, and temperature) on the removal performance of PANI and MO.
5. Test the adsorptive performance (adsorption isotherm studies) of PANI/MO towards Cu^{2+} and Pb^{2+} from wastewater.
6. To test the anti-micro-bacterial of PANI/MO on Staphylococcus Sps, and Bacillus Subtillis.

CHAPTER TWO: LITERATURE REVIEW

2.1 Ground Water

Approximately 30% of clean water in nature is groundwater, and 53% of the world's populations use groundwater as a source of drinking water. Water is one of the essentials that support all forms of plant and animal life, and it was generally obtain from two principal natural sources: surface water, such as freshwater lakes, rivers, and streams, and groundwater, such as borehole water and well water [12].

Groundwater is water that exists mainly in subsurface pore spaces but also in defined channels, such as those found in karst formations, which created by the dissolution of soluble rocks such as limestone. After the polar ice caps, groundwater is the next-largest reservoir of freshwater on Earth, containing more than 100 times the volume of streams and freshwater lakes [13].

2.2 Ground water contamination

Ground water contamination has become one of the main environmental issues today and it has been reported to contributed to serious health problems among many users. Ground water contamination can result from natural substances or anthropogenic activities that can cause disturbance of the natural materials or add contaminants to the existing ones. These contaminants include different naturally occurring chemicals and anthropogenic chemicals emerging from domestic and public wastes, industrial waste (organic, inorganic, trace elements etc.), mining activities (chemical, heavy metal elements, infiltration etc.). Degradation is the result of the development, use and reuse of water sources such as infiltration, over-pumping, seawater mixing, surface water contamination and rock-water interaction [14]. Chemicals used in water treatment such as pesticides which are used in water for public health purpose; cyanobacteria toxins and other contaminants derived from biological sources are also sources of water contaminants. Developments technologies have all affected the natural processes that determine the availability and composition of groundwater. According to WHO 80% of diseases are arises due to contamination ground water [12].

Heavy metal are one major groundwater pollutants which increased by human activities like mining, discharging industrial effluents containing metals without giving any treatment from industries like steel plants, battery, thermal power plants and over usage of fertilizers containing heavy metals in agriculture are the main reason to contaminate the ground water. Most people

living in remote areas of developing countries are largely dependent on groundwater as a source of drinking water. However, the groundwater could contaminate with various pollutants, such as heavy metal [5].

According to Kennish (1992), heavy metals are elements having an atomic weight between 63.54 and 200.59 and a specific gravity greater than 4 [14]. Heavy metal was collective applied to a group of metals (and metal-like elements) with a density greater than 5 g/cm3 and an atomic number above. Heavy metals, including copper (Cu), zinc (Zn), nickel (Ni), lead (Pb), mercury (Hg), cadmium (Cd), arsenic (As), chromium (Cr), etc. Heavy metals are major pollutants in the environment due to their toxicity and threat to creatures and humans at high concentrations [4]. Nowadays, due to fast-developing industrialization, water sources on Earth was become contaminated by different heavy metals more than their acceptable limit, which affects the ecological balance and human health [15].

Table. 1 The maximum acceptable concentrations of Cu^{2+} and Pb^{2+} in pure groundwater set by the Environmental Protection Agency (EPA).

Element	**EPA Limit (mgL-1)**	
Copper	1.3	[16]
Lead	0.005	[16]

Copper (Cu) is mined as a primary ore product from copper sulphide and oxide ores. Mining activities are the major source of copper contamination in groundwater. Other sources of copper include algicides, chromate, copper arsenate (CCA), pressure-treated lumber, and copper pipes. Lead pollution to ground water from natural factors include soil erosion, volcanic activities, urban run offs and aerosols particulate, while the human factors include metal finishing and electroplating processes, mining extraction operations, agricultural fertilizers, insecticides and pesticides textile industries and nuclear power. Around the world, many developed countries suffer from inadequate quantities of groundwater due to unpredictable climate changes resulting from the degradation of water sources, natural disasters, and the human population's rapid increase. These high-level heavy metals led to the poisoning of aquatic organisms via the bio-magnification of non-biodegradable metal ions inside the food chains [18, 19].

Table. 2 Acute and Chronic Effects of Cu^{2+} and Pb^{2+} on Human Beings.

Element	Acute	Chronic
Copper	Blue vomitus, GI irritation/ hemorrhage, hemolysis, metal fume fever (MFF) - inhaled Vomiting	vineyard sprayer's lung (inhaled); Wilson disease
Lead	nausea, vomiting, encephalopathy(headache, seizures, ataxia, obtundation)	encephalopathy, anemia, abdominal pain, nephropathy, foot-drop/wrist-drop

Removal of Cu^{2+}, and Pb^{2+} from groundwater achieved through chemical precipitation, ion exchange, ion floatation, adsorption, reverse osmosis, and membrane filtration. Among these conventional methods adsorption have a higher capacity for the removal of toxic Cu^{2+}, and Pb^{2+}. Moringa olifera was one of best adsorption that has low-cost adsorbents as a considerable potential solution for the removal and recovery of pollutants from rock leaching effluents [19].

2.3 Moringa Olifera

The Moringaceae, or horseradish tree, is a family of trees that consists of 13 different species, of which Moringa olifera is the most widely cultivated. Moringa is native to the sub-Himalayan parts of northern India, Pakistan, Bangladesh, and Afghanistan. Moringa is a multi-purpose food plant that originated was produce, and was use in many African countries, South America, and New Zealand. However, it has been cultivated in many parts of the world and now found in almost all tropical countries. M. olifera typically grows in semi-dry, desert, or tropical soils. Almost all parts of this plant root, bark, gum, leaf, fruit (pods), flowers, seed, and seed oil have been used for treating various ailments [19].

Moringa olifera (drumstick tree) is a rapidly growing deciduous shrub or small tree of about 13 m tall and 35 cm in diameter with an umbrella-shaped open cap. Moringa olifera is the most widely distributed species of the Moringaceae family throughout the world. It was report that Moringa olifera oil and micronutrients contain antitumor, antiepileptic, antidiuretic, anti-inflammatory, and venomous bite characteristics [19].

Various natural-based materials were studies as potential low-cost coagulants for water purification, including Moringa olifera (MO) seed. MO seed is one of the popular natural materials investigated, as it has shown ability to remove various heavy metals such as copper, nickel, zinc, and colour from ground water [5].

Figure. 1 Peeled of Moringa olifera seed

Obuseng et al. (2012) reported that the carboxylic acid and hydroxyl groups present in M. olifera play a major role in the removal of heavy metal ions, as observed from the significant reduction in the intensity or shift in their intensity peaks for metal-loaded samples by using a Fourier transform infrared spectrophotometer. They also reported that the trend of heavy metal removal using the sonication method followed the order Pb > Cu [20].

The seeds of Moringa olifera were consider lignocellulose adsorbents due to their cellulose, hemicellulose, and lignin constituents. Seeds that contain 30% and 30% lipids were made-up of functional groups such as O-H, C-O, and C-N, which comprise macromolecules. Amino acids are a major constituent of the functional group. The proteinases amino acids have diverse structures in relation to pH-dependent properties and consist of physiological groupings of varying binding agents. The binding agents have a great ability to interact with a metal either by metal ion exchange or by complexation to form an organo-metallic complex. Moringa olifera seed (MOS)-metal ion binding appears to be an ion exchange process involving electrostatic attraction between negatively charged groups of amino acids and metallic cations [21].

Moringa olifera seed (MOS) coagulant traditionally used for water purification. Moringa olifera peeled seed recommended as a good coagulant for turbidity and heavy metal removal. Previous

studies by the author show the potential of Moringa olifera (MO) as a coagulant, clarifier, and adsorbent [22].

The binding agents have a great ability to interact with a metal by either metal ion exchange or complexation to form an organo-metallic complex. Moringa olifera seed (MOS)-metal ion binding appears to be an ion exchange process involving electrostatic attraction between negatively charged groups of amino acids and metallic cations. However, moringa olifera is less efficient at removing toxic heavy metals from wastewater. Surface modification using conductive and active materials is required to enhance its adsorption performance [23].

To improve further on the previous studies, a new composite medium will be prepared by using moringa olifera biopolymer and PANI. The advantages of these materials are their natural abundance, non-toxicity, environmental friendliness, and cost effectiveness [22].

2.4 Polyaniline

The interest in electrically conducting polymers continues to rise rapidly, with the wide range of applications. The motivating force for ongoing research in this field is the potential for a variety of electrical properties combined with advantages of polymers, for instance, light weight, the relative ease in processing and chemical resistance. Conducting polymers are widely used for various applications, including actuators, sensors, electromagnetic interference (EMI) shielding, electronic nanodevices, fuel cell, supercapacitors. Great efforts have made during the past two decades in the understanding of the structural, electrical, chemical and optical phenomenon of these polymers, such as polypyrrole (PPy), polythiophene (PT), polyaniline (PANI), polyphenylene (PPh) and their derivatives. Among these polymers, PANI has been the center of focus during the last decade due to the presence of reactive NH- groups in its polymer chains, interesting redox properties, low-cost monomer, facile synthesis and good electrical conductivity.

Polyaniline commonly abbreviated as PANI or Pani also known as aniline black discovered for the first time by Ferdinand Runge in 1834 from the initial oxidation of aniline. Later, in 1862, Henry Lether achieved the first electrochemical polymerization. Since then, it has applied to a variety of coloured materials and dyes. Recently, PANI has gained much attention in the scientific community due to the rediscovery of its conductive properties in the 1980s. Its structure consists of a succession of aromatic rings of the benzene di-amine or quinone di-imine

types, bridged by a nitrogen heteroatom. PANI has three oxidation states that are represented in Fig. 2 fully reduced leucoemeraldine base (LB), fully oxidized pernigraniline base (PB), and half-oxidized emeraldine base (EB), which is converted to emeraldine salt via protonation with organic and inorganic acids [9].

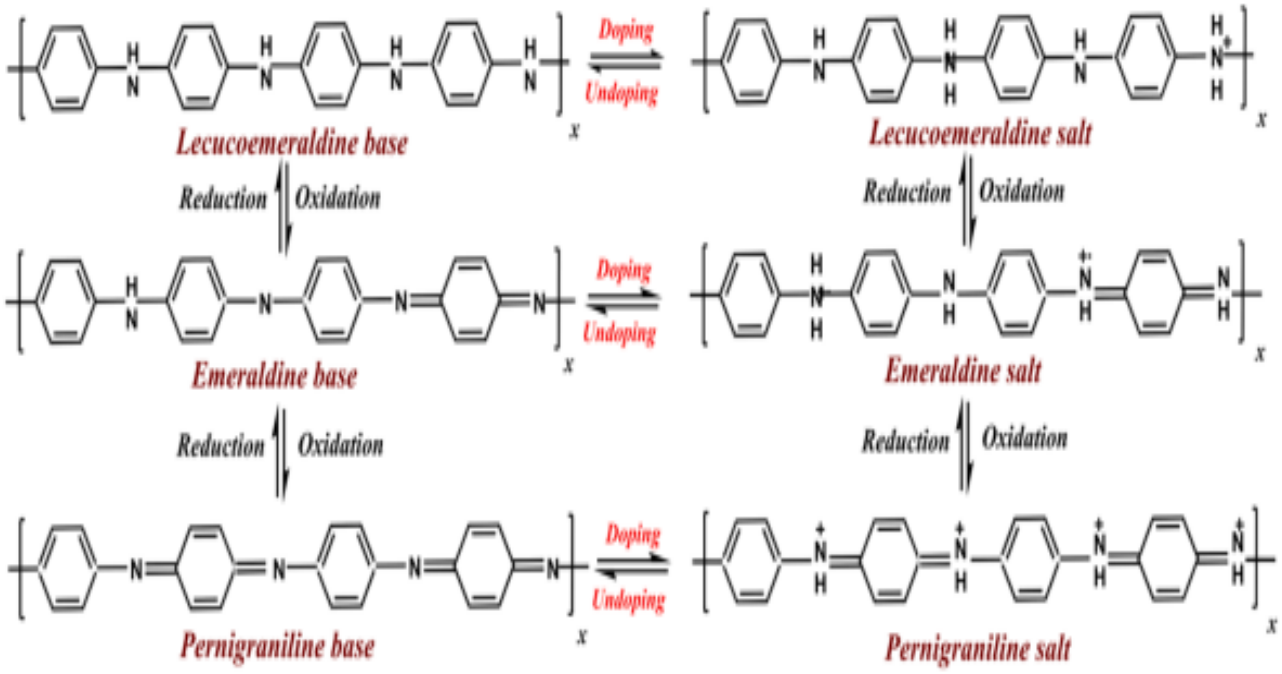

Figure. 2 Different configurations of PANI structures

In 1862, Lethe prepared it through the oxidation of aniline under mild conditions. Attempts to control the synthesis conditions of polyaniline grew until the 1910s, when Green and Woodhead managed successfully to control the conditions, which led to the discovery of its four-oxidation states. Jozefowic's group followed this in the 1960s and 1970s for a better understanding of the material. After this, the study of polyaniline with other ICPs (intrinsic conducting polymers) increased worldwide and studied for different applications. However, engineering applications of polyaniline are restricted because of poor processability in common solvents, aggregate formation, and low mechanical strength. In order to exploit the fascinating features of polyaniline, various approaches was test, including doping with functionalized protonic acids, blending with other polymers, and coating fibrous materials. These processes offer improved process ability, reduced aggregation, and better mechanical strength for polyaniline [10].

Gu et al. reported the synthesis of Fe_3O_4/PANI nano-composites for the removal of heavy metals from groundwater. The microstructure characterization showed that the nano-composites' surface became rougher, and a thin PANI layer was observed surrounding the Fe_3O_4 NPs. After adsorption of heavy metal, the nano-composites exhibited similar magnetic properties, confirming that PANI effectively protected the Fe_3O_4 NPs from dissolution, although a slight decrease in the specific surface area was observe. However, they show poor performance when used as adsorbents for the removal of heavy metals because of the challenge of separating them from aqueous solutions and reusing them, and they are susceptible to acid conditions, air oxidation, and aggregation in aqueous systems. In another study, Fan et al. reported the synthesis of a three-dimensional polyaniline graphene oxide (PANI/GO) material for the removal of heavy metals from groundwater. The prepared material exhibited a loose and spongy macro-scale porous structure, with sponges showing a rough and shaggy structure with numerous pores. However, they show poor performance when used as adsorbents for the removal of heavy metals because of the challenge of separating them from aqueous solutions and reusing them [9].

A PANI/SiO2 nanocomposite synthesized via the in situ polymerization of aniline monomers on the surface of commercial SiO2 nanoparticles. Ion exchange and adsorption-coupled reduction were the main mechanisms of heavy metal adsorption onto PANI/SiO2. However, the significance of these materials arises from their pore sizes, which allow controlled accessibility to large molecules depending on pore geometry [9].

Polyaniline was produce by oxidative polymerization, chemical or electrochemical, of aniline. Standardization of polyaniline synthesis to obtain unique electrical properties has always been a challenge, and thus a vast range of conductivity values, varying from below 0.5 S/cm to over 300 S/cm, was report in the literature. Several factors, such as the choice of oxidizing agent and ratio of amounts of oxidizing agent and aniline, doping, polymerization temperature, and so on, was shown to affect its conductivity and yield [24].

The application of PANI for wastewater treatment has been widely studied owing to its exceptional structure, which comprises abundant amine and imine functional groups. The nitrogen atoms in these functional groups have lone pairs of electrons to facilitate chelation and adsorption of pollutants. However, PANI has limitation such as poor mechanical properties and processing ability, as well as low solubility. These limitations emanate from its high conjugation

and strong electrostatic interaction between chains, which decrease its performance and limit its commercial application. On the other hand, the large swelling, cracking, shrinking, acidity, and low adhesion problems during the charge discharge process often disrupt the mechanical stability of PANI. Therefore, PANI was coat on the surface of MOS materials utilized to support the mechanical structure and improve the electrochemical stability of PANI due to the synergetic effect between PANI and MO [25, 26].

2.5 Physical and Chemical Properties of Polyaniline

The inherent features of conducting polymers have attracted considerable attention from scientists and researchers. Polyaniline is among such polymers, which commonly used for chemical sensors and electrical and electronic devices. It is made up of benzoin (-B-NH-B-NH) n and quinoid (-B-N=Q-N=) n repeating structures. A Polyaniline structure was varies by variation in the ratio of oxidation-reduction states of amino groups (doping). These structures include fully reduced leucoemeraldine, completely oxidized pernigraniline, and partially oxidized emeraldine forms. These structures were switch from one form to another by simply changing chemical environments and stimulants, thus creating an opportunity to produce smart biomaterials, sensors, and electronic devices [10].

2.6 Synthesis of polyaniline

Two most commonly used synthesis routes are chemical and electrochemical polymerizations. Each method has its own strengths and limitations. As a result, selection of polymerization method is dependent on the intended application. For instance, electrochemical reaction provides a film deposited on the electrode material with controlled thickness and morphology. It is very pure compared to chemical oxidation, as it employs no catalysts. For this reason, the output is preferably using in electronic devices requiring high electrical conductivity. While chemical polymerization is classic with the cost and ease of production for bulk quantities within short period of time [10].

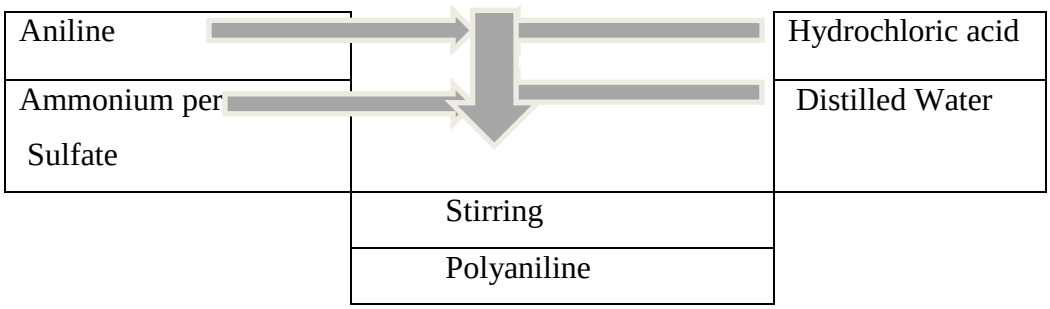

Figure 3 Flow chart of the experimental step

Conducting polymers show unusual electrochemical properties like high electrical conductivity, low ionization potential, high electronic affinities, and optical properties. These properties are only because of conjugated electron backbones in CP. There must be high degree of overlapping of the polymer molecular orbital, which permits the formation of a dislocated molecular wave function and partial occupation of the molecular orbital if there is to be free movement of electrons throughout the lattice. Conducting polymers exhibit intrinsic electronic conductivity ranging from about 10^{-4} to 10^{2}S cm^{-1} due to extension of the doped state [27].

Chemical polymerization of aniline is facilitating by addition of several catalysts and initiators like the most commonly used iron (III) compounds and ammonium peroxodisulphate. Iron (III) chloride salts (E_o= 0.771V) are weaker and cheaper oxidants. Consequently, it is more preferable over counterpart ammonium peroxodisulphate (E_o= 2.01V). Polyaniline synthesized using ammonium peroxodisulphate shows a little higher electrical conductivity. However, formation of colorful and water-soluble filtrate makes it undesirable oxidant and environmentally unfriendly. There are also other supporting evidences that proved ammonium peroxodisulphate initiates side reactions which are associated with strong oxidizing nature [10].

Nevertheless, the insulating state of virgin polyaniline could remarkably change to semiconductor or metallic state through doping phenomenon. Doping is a reversible process, which simply generates conjugation defect on the polymer backbone forming polarons or bipolarons stabilized by counter ionic species. Besides to increasing conductivity, increasing level of doping also enhances solubility and process ability of polyaniline depending on the functional groups that exist within the dopant structure. Protonic acid dopants containing different functionalities such as carboxyl and sulphonate groups facilitate solubility and process ability of polyaniline [14].

2.7 Factor Influencing Adsorption on Chemical Deposition of Polyaniline Surface Moringa Oliefera Seed Removal Heavy Metal in Wastewater

In recent years, PANI nano-particle was use as adsorbents for the removal of various pollutants from wastewater. More studies were focuses on the adsorption of heavy metals ions due to their good interaction with PANI nano-composites functional groups. In my study of interaction between PANI with MO, various adsorption parameters such as pH, contact time, adsorbent dose, and temperature, nature of the adsorbent and concentration of the pollutants were investigates. From these parameters, the efficiency and adsorption capacity of PANI/MO was determined to confirm the potential of the adsorption capacity for water purification [22].

2.7.1 Effect of pH on Adsorption

Most of the metal adsorbed increase with the increasing of pH of the solution until certain point and followed by reduction if further increasing of pH [28]. Furthermore, the presence of a significant number of H^+ or HO^- ions in water competes with metal ions for adsorption. At a moderate pH, the rate of adsorption rises because electrostatic repulsions are reducing due to deprotonating of the active sites. Several other investigations have found that adsorption of heavy metal ions is better at moderate pH levels than at lower pH levels [15,22].

2.7.2 Effect of Contact Time

The interaction of functional group between the solution and the surface of adsorbent result in the adsorption capacity if adsorbate into adsorbent. Specific time needed to maintain equilibrium interaction therefore the adsorption process undergo completion[28]. It was find that the rate of adsorption increased with an increase in the time of reaction until the equilibrium was obtain between the number of adsorbents and the number of sorbets that remain in the solution. In general, adsorption occurred quickly in the preliminary phases and steadily slows down as the equilibrium state occurred between metal in the liquid and solid phase [3,22].

2.7.3 Effect of Temperature

The natures of the processes either exothermic or endothermic are depends on the adsorption equilibrium that affected by the temperature used. The uptake capacity of the adsorbate increases with the rises of the temperatures. This happens due to the enlargement of pores and activation of the sorbent surface [28].

2.7.4 Effect of Sorbent Dose

Dose of adsorbent also is one of the main points to determine the capacity uptake of heavy metals by adsorbents. Usually, increase in the dose of adsorbents will increase in the adsorbed capacity until its reach a limit. If further increase the dose, the adsorption capacity will be constant. Wang study adsorbent loading from 0.5 g until 2.0 g, removal of copper increase with increase of adsorbent loading [28]. With an increase in sorbent amount, the percentage of metal extraction increases. This may be due to the presence of sorption space, to which adsorbate will bind. The determination of adsorbent dose provides an idea regarding the least amount of sorbent requires for the sorption process [3,22].

2.7.5 Effect of Initial Concentration

Adsorption dosage gains a strong effect by initial concentration of heavy metals. Generally, adsorption capacity increased with the increased initial concentration of heavy metals. Playing as important driving force, initial concentration influence in overcome all mass transfer resistance between solid and aqueous phases. Several studies have shown that removal efficiency of heavy metal is concentration dependent and there exist decreasing trend if further increase initial concentration [28].

2.8 Application of PANI/MO Nano Composite as Adsorbents for Wastewater

2.8.1 Adsorption of Heavy Metal

The general sources of heavy metals are weathering of rocks due to their abundance in nature and mining industries because of mineral process of metal ores. Various heavy metals known to pollute water include nickel, cadmium, lead, and mercury, chromium, arsenic and copper. The water pollution by these toxic metals is a global concern owing to their acute toxicity and enduring accumulation. Heavy metals are problematic since they are mutagenic, carcinogenic, are not biodegradable and can form various species [11,22].

2.8.2 For Anti-micro-bacterial Test

The application of flexible polymer nano-composites for food packaging to inactivate microorganisms associated with foods is the demand of the present-day food industry to assure quality throughout the packaging operation. The discoveries of antimicrobial drugs are necessary, as the pathogens become resistant to already existing drugs in vogue. Polymers with

antimicrobial properties are widely employed in the fields of health care, pharmacy, food packaging and tissue implants. Among the various types of polymers, conducting polymers are of great interest in biomedical applications due to good cellular response. In addition, they have antimicrobial activity as growth inhibitors, killing agents and antimicrobial carriers. PANI/MO was the ability to control pathogenic Bacillus Subtillis and staphylococcus aurous [44]..

CHAPTER THREE: METHODOLOGY

3.1 Materials

3.1.1 Chemicals and Reagent

The following reagents were used for analysis and synthesis, aniline (Aldrich, 99.5%, England), hydrochloric acid HCl-37% Merck)), ammonium peroxydisulfate (APS-98% Merck)), acetone, dimethylsulfoxide (DMSO-99% Aldrich, Germany), Copper sulphate (99%), lead nitrate (99%), Copperon, and LeadTrak, distilled Water. They were all analytical reagent grade and used without further purification

3.1.2 Apparatus and Instruments

The apparatus and instruments that were used includes: pipette, quartz cuvette, electronic balance, beaker, magnetic stirrer with hot plate, conical flask, volumetric flask and funnels, measuring cylinder, filter paper, crucible, mortar and pestle, dropper, beaker and, XRD(XRD-7000 SHIMDAZU Corporation Japan), FTIR(IS-50-ABX), SEM(ISM-6000+SEM SHIMADZU Corporation, Japan) and UV/Vis Spectrophotometer(Ach DM-6000) instruments was used.

3.2 Methods

3.2.1 Description of Study Area

This research study was conducted at Enamor Woreda Gurage Zone, located in SNNPR, Ethiopia. Wolkite was a town and separate Woreda in southwestern Ethiopia, 158 km from Addis Ababa, capital city of Ethiopia. Wolkite is administrative center of the Gurage Zone of the Southern Nations, Nationalities and Peoples' Region (SNNPR); these towns have a latitude and longitude of 8°17′N 37°47′E and an elevation between 1910 and 1935 m above sea level. Four wastewater samples of the were collected, two from Torhegn kebele, one from Worket Elementary School and one from Gubre town of Gurage Zone, Ethiopia. The location map of the study area is shown in **Figure 4** below.

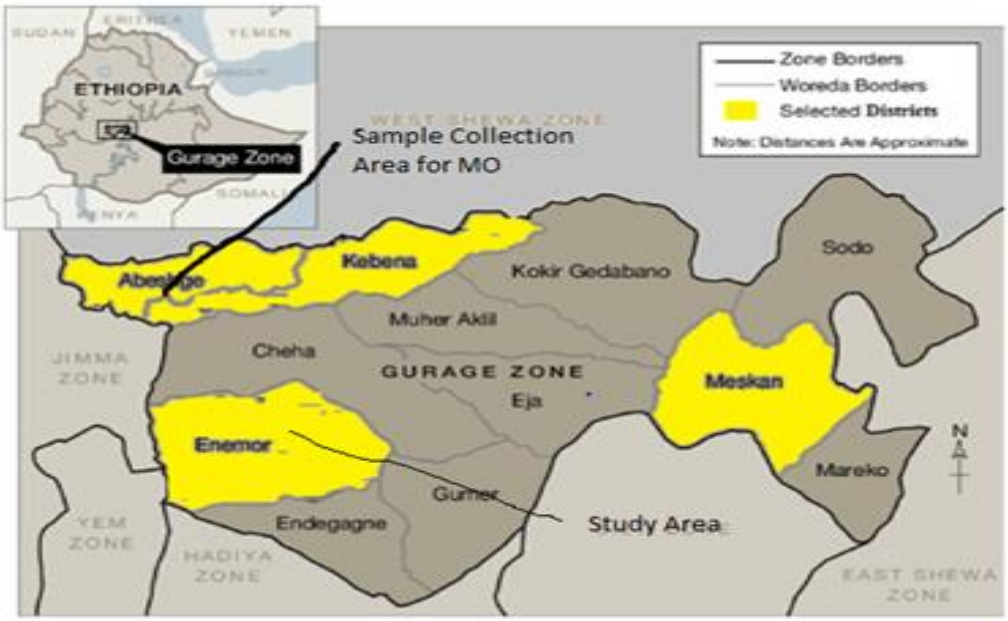

Figure. 4 Map of Gurage Zone show sampling source.

3.2.2 Water Sampling

Totally, of four ground water samples were collected by pre-cleaned and rinsed polythene bottles of two-liter capacity with necessary precautions.

3.2.3 Sample collection, preparation, and analysis

According to the field survey conducted in the sampling area, ground wastewater generates from its various activities such as agriculture, decomposing rock, mining activities, landfill, toilet, sewage, and over pumping. This might cause harmful effects to the environment and human health, including undesirable changes to ecosystems and human health risks. Thus, sample collection was carried out after the field survey has been completed. The method of sampling a random depth integrated sampling and a total number samples four representative ground wastewater samples were collected. Therefore, wastewater samples of the were collected, one from Torhegne health center, one from middle Torhegne, one from Worket Elementary School, and one from Gubre town of Gurage Zone. The collected wastewater samples were stored at a temperature below 4 °C in refrigerator before laboratory analysis.

3.2.4 Procedure for physicochemical analysis

The physicochemical parameters such as, Temperature, and pH were measured onsite. These parameters were measured by digital pH-meter by initially calibrated with known standard buffer

solution with a pH value of 4, 7and 10 following the procedures given on the instruction manual. The pH of all water samples was measured onsite. The temperature of all water samples was measured by using portable thermometer onsite. Turbidity was calibrated with standard solution of 400NTU. using Hydrazine Sulphate and Hexamethylenetetramine, then turbidity water sample was measured. Total Suspended Solids (TSS) was measured by filtering 50 ml of water sample through Whitman~ 41-filter paper. Total dissolved solid was measured by evaporation 50 ml water sample through Evaporating dish. For the determination of Hardness, 50 ml of sample was buffered at pH 8 -10 (NH_4Cl and NH_3), and titrated against standard EDTA using Erichrome Black T as indicator. The totals Alkalinity were measured by titrating the sample against N/50 solution of hydrochloric acid using methyl orange indicator. Chloride content was measured by titrating against N/50 solution of silver nitrate using potassium chromate as indicator.

3.2.5 Digestions of wastewater Samples for Heavy Metal Determination

Acid digestion using 69 % nitric acid were performed to destroy organic matter and to dissolve larger particles in the sample, thus allowing determination of the total concentration of metals. A final addition of 2mL of nitric acid was added to the all sample in order to dissolve any remaining particle [19].

3.2.6 Sample Analysis

All the ground waters were analyzed by UV-visible spectrometer. The pH of the ground waters was measured using pH and temperatures in site and in the laboratory.

Table. 3 Instruments or methods used for the determination of physicochemical parameters and Characterization of PANI, MO and PANI/MO nano-composite and site at which analysis were performed.

Parameters	**Method**	**Site**
pH	Digital pH meter	WKU
EC	DDS 307 meter	WKU
Temp	Thermometer	WKU
TDS	Evaporation	WKU
TSS	Filtration	WKU
Turbidity	Haffmans Vos Rota 90-90/25	WKU
Hardness	Titration	WKU
Alkalinity	Titration	WKU
Cl^-	Titration	WKU
Pb and Cu	UV-Vis (HACH DR 6000)	Zabidar brewery S.C
MO PANI PANI/MO	SEM JSM-6000 PLUS, SHIMADZU corporation Japan	ASTU
	XRD-7000, Shimadzu	AAU 4 kilo Campus
	S50ABX FT-IR spectroscopy	AAU 6 kilo Campus
	UV- Vis (JASCO V-770)	AAU 6 kilo Campus

3.2.7 Sample preparation

Moringa oliefera seed were collected from Abashige wereda Wudad 5 kebele, in South Nation Nationalities people of Ethiopia (SNNPE) Region, in Gurage zone. The MO seed was clean and rinsed with distilled water, and dried in an oven at 100 ºC for 1 hour. The moringa seed was ground to a fine powder, and sieved through a stainless steel mesh with an opening size of 300μm to obtain MO particles of similar size.

3.2.8 Synthesis of Polyaniline

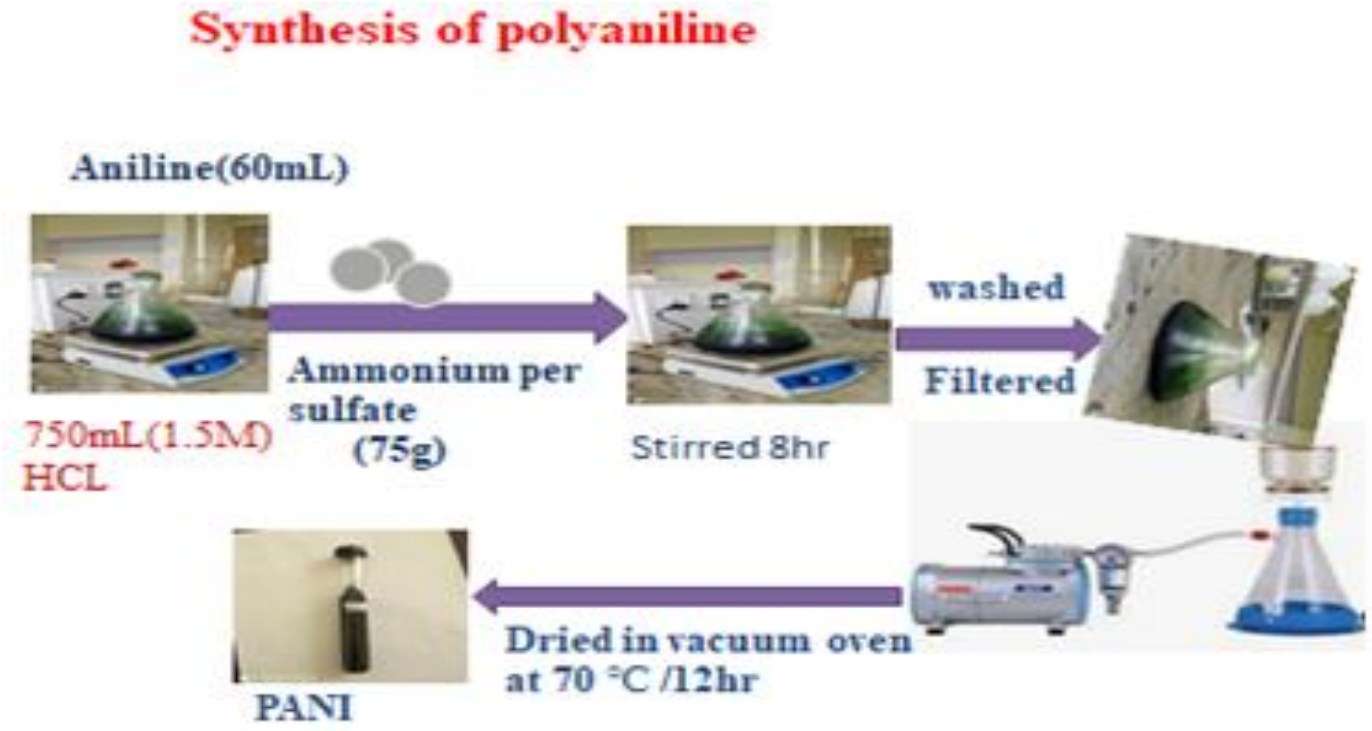

3.2.9 Surface Coating of Polyaniline on Moringa Oliefera

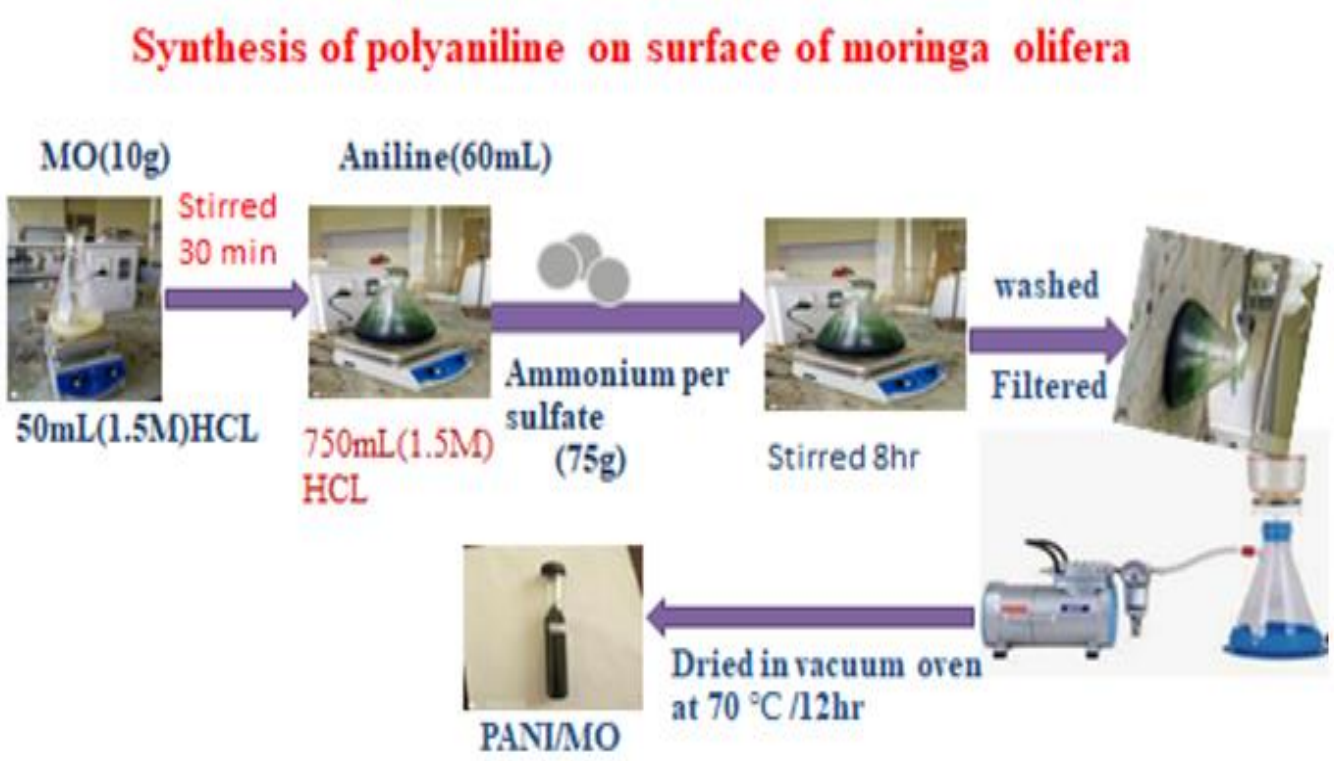

3.3 Characterization

3.3.1 UV-Visible spectroscopy

UV/Vis Spectrophotometer(Ach-6000) was to measure initial and finally Cu^{2+}, and Pb^{2+} in wastewater. Stock solution prepared from each standard at different concentrations is use to get calibration curve for each metal [31].

3.3.2 Color Fastness Tests Coupled with UV–Visible Spectroscopy

MO, PANI, PANI/MO was soak in distilled water separately and subjected to color fastness test in Mesdan Auto Wash with a speed of 40 rpm at 68 ^{0}C for 90 min washing time [31].

3.3.3 Fourier Transforms Infrared (FT-IR) Spectroscopy

An FTIR (IS-50-ABX) spectrum were useful for identify functional groups that attached to a certain surface. FTIR were using to record the spectra of MO, PANI, and PANI/MO samples were analyzed the chemical structure. KBr disk technique were used in a spectral range of 4000-400 cm^{-1} [31].

3.3.4 X-ray Diffraction (XRD) Analysis

X-ray diffraction studies were performed under ambient condition on X-ray diffractometer (XRD-7000 SHIMDAZU Corporation, Japan) radiation with 40 kV and 30mA on rotation between 10^0 to 70^0 at 2θ scale. XRD analysis were used to examine the structure of MO, PANI and MO/PANI [31].

3.3.5 Scanning Electron Microscopy (SEM) Analysis

Surface of Moringa Olifera (MO), PANI, and polyaniline coated moringa olifera (PANI/MO) were determined using a highly customizable scanning electron microscope (ISM-6000+SEM SHIMADZU, Corporation, Japan) coupled with a port for analytical attachment of energy dispersive X-ray (EDX) spectrometry [31].

3.3.6 Electrical Conductivity Studies

Electrical conductivity(DDS-307) of PANI, and PANI modified MO were measured using portable conduct meter device by dissolving in deionized solution[31].

CHAPTER FOUR: RESULT AND DISCUSSION

4.1 Determination of physic-chemical parameters

The statistical summaries of the physic-chemical parameter of wastewater samples taken from three different sampling sites Gubre(G), Worket Elementary School(WES), Middle Torhegne(MT), and Torhegne Health Center(THC) (Mean ± SD, n=4) were investigated. The results are presented in

Table .4 The average values of various parameters analyzed in each sampling site, such as pH, temperature, turbidity, electrical conductivity, total dissolved solids, total suspended solids, total alkalinity, total hardness, chloride ion concentration.

Parameter	**G**	**WES**	**MT**	**THC**	**WHO**
pH	6.49 ± 0.01	6.96 ± 0.01	6.88 ± 0.01	7.18 ± 0.021	6.5-8.5
Cond(µs/cm)	54 ± 0.817	165.67 ± 1.25	151.9 ± 0.082	165.8 ± 0.1	250 µS/cm
T °C	22.6 ± 0.082	22.7 ± 0.082	22.57 ± 0.094	22.63 ± 0.152	15-20^{o}C
Turb (NTU)	22 ± 0.817	18.83 ± 0.62	22.5 ± 0.408	21.5 ± 0.5	<10NUT
TSS (mg/L)	51 ± 0.817	59.8 ± 0.624	71 ± 0.817	81.7 ± 1.5	≤ 30 mg/L
TDS (mg/L)	40 ± 0.356	114 ± 0.817	98.17 ± 0.624	108.8 ± 0.1	500mg/L
TA (mg/L)	102 ± 1.25	420 ± 21.60	320 ± 16.33	303 ± 6.08	500 mg/L
TH(mg/L)	105 ± 2.63	421.15 ± 82.53	410 ± 8.17	373.3 ± 25.17	1000mg/L
Chloride	74.5 ± 0.64	135 ± 0.82	115 ± 4.08	120 ± 5	<250 mg/L

4.1.1 pH

Determination of pH was very important because it influences the other physicochemical parameters and the availability of metal ion in the water. The pH value range from 6.49 to 7.17 indicates slightly acidic in nature and in addition, all the biochemical reactions are sensitive to the variation in pH and it is one of the most important operational water quality parameters. The maximum pH was recorded as 7.2 at sampling location Torhegne health center and minimum was 6.49 (Gubre) which is beyond the maximum permissible limit which is slightly acidic. When composed with the standard values of WHO and IS 10500-91, the samples are found to be in the permissible limit as prescribed.

4.1.2 Temperature

The temperature of water and wastewater is one of the most important characteristics that determines, to a considerable extent, the trends and tendencies of changes in the ground water quality. Temperature is an important biologically significant factor, which plays an important role in the metabolic activities of the organism. This might be due to presence of the effluents. Our property of water was that with change in temperature, its density varies and it becomes less with warming up and more with cooling. At above 32°C, it would be considered "unfit" for public use. Therefore, temperatures of all water samples are between the standard value by WHO.

4.1.3 Turbidity

In most ground water, turbidity is due to colloidal and extremely fine dispersions. The turbidity values varied between 19.45 NTU (WES) to 22.9 NTU (MT). Turbidity of total investigated samples, 50% water samples shows greater value than the limit prescribed by WHO. There was a risk pathogenic organisms could have shielded by the turbidity particles and this indicate that it is necessary to treat water from this sampling area for using.

4.1.4 Electrical Conductivity

Electrical Conductivity is the measure of capacity of a substance or solution to conduct electric current. EC values were in the range from 54.82μS/cm (G) to 166.92μS/cm (WES). EC values for all the investigated samples were found to be below the limit prescribed by WHO.

4.1.5 Total Dissolved Solid (TDS)

Water containing more than 500 mg/l of TDS does not consider desirable for drinking water supplies, though more highly mineralized water has used where better quality water is not available. TDS values were in the range from 40.4mg/L (G) to 108.9mg/L (THC). The TDS values of all the water samples of the selected places are below the limit prescribed by WHO and IS-10500-91.

4.1.6 Total Suspended Solid (TSS)

The result indicates sample which have high TSS value may have high contamination and this may introduce different diseases which affect all living things. Suspended solids are closely linked to nutrient transport (phosphor, especially), metal, industrial waste and chemicals used in agriculture transport. Regarding the values of TSS, all the water samples showed excess presence

of contaminants, and the standard value TSS were in the permissible limits of WHO (≤ 30 mg/L). The TSS result indicates all water samples that have high value by WHO, this may have high contamination and this may introduce different diseases, which affect all living things.

4.1.7 Total Alkalinity

Total alkalinity is a measure of the ability of water to neutralize acids. The alkalinity of groundwater is mainly due to carbonates and bicarbonates. The highest value of alkalinity has found as 441.6 mg/L at sampling location (WES) and lowest 103.25mg/L at (G). The acceptable limit total alkalinity in ground water of is up to 500 mg/L by WHO. TA value in below the standard of limit by WHO.

4.1.8 Chloride

Chloride in surface and groundwater from both natural and anthropogenic sources, such as run-off containing road de-icing salts, the use of inorganic fertilizers, landfill leachates, septic tank effluents, animal feeds, industrial effluents, irrigation drainage, and seawater intrusion in coastal areas. A chloride range of 200 mg/L for groundwater was considered standard value by WHO. The result of chloride ion in all water samples was below the standard value of WHO.

4.1.9 Total Hardness

Hardness is one of the very important properties of ground water from a utility point of view for different purposes. Total Hardness was found in the sample water ranges from 107.67mg/ (G) to 503.68 mg/L (WES). According to some classifications, water having hardness up to 75 mg/L us classified as soft, 76-150 mg/l is moderately soft, 151-300 mg/l as hard and more than 300 mg/l as very hard. On this basis, the results show that samples from (G) were moderate soft, sample from (THC,MT,WES) very hard. Therefore, as the result investigated that it is necessary to treat water from this three sampling area before use.

4.2 Statically Data Analysis

4.2.1 Correlations

In this study the correlation coefficients (r) among various water quality parameters have been calculated and the numerical values of correlation coefficients (r) are tabulated in (**Table.5**).

Table .5 Correlation Coefficient (r) of Physico-chemical parameter, and heavy metal of wastewater samples.

Correlation	PH	EC	TUR	TSS	TDS	TA	TH	Temp	Cl^-	Pb	Cu
PH	1										
EC	.932**	1									
TUR	-.004	-.089	1								
TSS	.880**	.752**	.433	1							
TDS	.922**	.996**	-.168	.703*	1						
TA	.766**	.927**	-.307	.469	.949**	1					
TH	.781**	.944**	-.259	.511	.959**	.993**	1				
Temp	.422	.388	-.159	.197	.428	.500	.454	1			
Cl^-	.848**	.958**	-.284	.567	.976**	.984**	.984**	.546	1		
Pb	.899**	.846**	.219	.837**	.829**	.719**	.731**	.589*	.782**	1	
Cu	.750**	.624*	.616*	.942**	.568	.363	.407	.319	.460	.825**	1

**. Correlation is significant at the 0.01 level (2-tailed).

*. Correlation is significant at the 0.05 level (2-tailed).

Pearson correlation coefficient was used examine the relationship between the various physic-chemical parameters in the water sample from all the sample sites. According to the researcher reported at high correlation coefficient (near +1 or -1) means good relationship between two variable and its concentration around zero means no relation between them at significant level of 0.05% l it can be strong correlated , If r=0.7, whereas r value between 0.5 and 0.7 shows moderate correlation between two different parameters[11]. Therefore, Pearson correlation coefficient matrixes among the determined physico chemical parameter are present in Table 4.2

PH was strong correlation between Pb(r=0.899), Cu(r=0.750**). The electrical conductivity of water depends upon the concentration of ions and its nutrient load. EC is a measure of capacity of a substance or solution to conduct electricity. It is an excellent indicator of total dissolved solids which is a measure of salinity which affects taste of potable water. EC shows significant

strong correlation with PH(r=0.932**), TDS(r=0.996**), TA(r=0.927**), TH(r=0.944**), Pb(r=0.846). While EC moderate correlation with Cu(r=0.624*), and weak correlation with Temp(r=0.388),

Cl^- significantly strong correlation with PH (r=0.848**), EC (r=0.958**), TDS (r=0.976**), Pb(r=0.782), TA, & TH (0.989**). While Cl^- moderate correlation with Temp (r=0.546), TSS (r=0.567), and weak correlation with Cu(r=0.460). TA shows significant strong correlation with PH (r=0.766**), TDS (r=0.949**). While TA shows significant weak correlation with Turb(r=0.307), TSS (r=0.469), Cu(r=0.363).

Total hardness significantly strong correlation with PH (r=0.781**), TDS (r=0.959**), TA (r=0.993**) Pb(r=0.719). While hardness showed weak correlation with Cu(r=0.407), Temp(r=0.454). TDS shows significant strong correlation with PH (r=0.922**), TSS (r=0.703**), Pb(r=0.821), TDS show moderate correlation with Cu (r=0.568), and weak correlation with Turb (r=0.168) Temp(r=0.428). TSS shows significant strong correlation with pH (r=-0.880**), EC (r=0.752**), Pb(r=0.837), Cu(r=0.942**), While TSS shows significant moderate correlation with TH(r=0.511), Cl^-(r=0.500), and weak correlation with Turb(r=0.433).

The suspended particles, soil particles, discharged effluents; decomposed organic matter, total dissolved solids as well as the microscopic organisms increase the turbidity of water, which interferes with the penetration of light. Turbidity shows negative significant correlation negatively correlated with PH (r=-0.004), EC (r=-0.089), TDS (r=-0.168), TA (r=-0.307), TH (r=-0.259), Temp(r=-0.159) Cl^-(r=-0.284).

4.3 Fourier Transform Infrared (FT-IR) Spectroscopy

Fourier-transform infrared (FT-IR) spectra of moringa olifera, polyaniline, and polyaniline-moringa olifera adsorbents in the doped was shown in **Figure 5**.

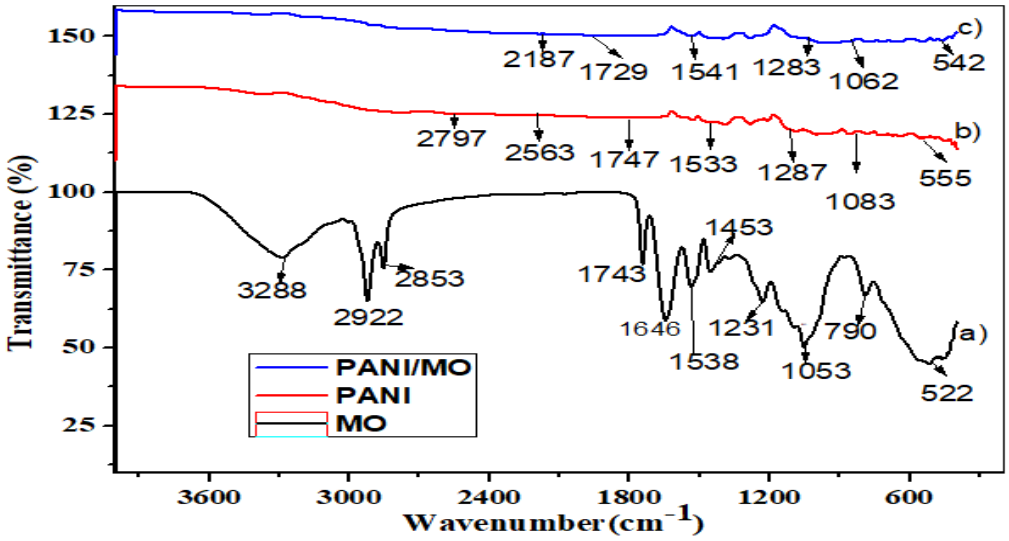

Figure. 5 FT-IR spectra of a) MO b) PANI and c) PANI/MO

Fig .5 (a) FTIR spectrum of moringa olifera peeled seed. FT-IR analyze was essential to identify functional groups present in the MO structure. Specifically, several proteins, lipid and polysaccharide structures, containing amine, hydroxyl, carboxyl, and carbonyl groups are found in Moringa olifera seed, common in lignocellulose MO. Due to the high content of protein present in seeds there was also a contribution in this region from the N-H stretching of amide groups [31]. The collected IR spectrum of the appears with IR features including the collective vibrational bands due to moringa olifera superimposed and extending from 400-4000 cm^{-1}. The FTIR spectrum of (**Figure. 5a**) shows broad stretching peak at 3288.82cm^{-1} corresponding to the stretching vibration of the N-H bond of amino groups and indicative of bonded hydroxyl group. The peak at 2922.64cm^{-1} and 2,852cm^{-1} was due to symmetrical and asymmetrical stretching of the C-H of CH_2 group present in fatty acids. The peak at 1743.64cm^{-1} primary amine group contained CO stretching. The carbonyl group was present in the fatty acid and protein structures. The peak at 1646.80cm^{-1} was due to (C=C vibrations in the phenyl Stretch) associated with the amide group in the protein[33]. The presence of a peak at 1,587 cm^{-1} was due to C-N stretching deformation. While peaks around 1231.22 and 1375.49cm^{-1} are due to C-OH stretching vibrations, 1143.51cm^{-1}, the intense band appeared at 1053.80cm^{-1} was due to C-O of alcohols

and carboxylic acids and confirms the lignin structure of Moringa oliefera, and 1094.26cm^{-1}(C-O-C bonding of alkoxy group), 522.36, 790.67, 477.88 cm^{-1} aromatic C–H out-of-plane bending vibrations [34]. The presence of this band confirms the protein structure in the Moringa seeds. Therefore, MO was observed that the Moringa olifera seed has amide, amine, carboxylic acid, hydroxyl and other functional groups, which possibly confirmed the presence of most of the necessary functionalities. Therefore, the functional groups like O-H, C-N, N-H and C-O are possibly playing their role in adsorption phenomenon by developing some electrostatic-forces or complexation between the functional groups on adsorbent surfaces and PANI. In (**Figure.5b**) FTIR spectra of the pure PANI were obtained in the transmission range 400-4000cm^{-1}. The IR spectrum of the synthesis PANI salts occurred at 3383, 2797, 2563, 1747, 1533, 1287, 1083, and 555cm^{-1}. The peak around 3383cm^{-1} was due to the stretching vibration of N-H bond for polyaniline molecular chain the secondary amine of the synthesized PANI salt[35]. The peak at 1325cm^{-1} was due to the C-N stretching mode[36]. The absorption peaks of 1,561 and 1,493 cm-1 was due to C=N and C=C stretching mode of vibration for quinine and benzenoid units of PANI. The absorption peak around 1400 cm^{-1} was attributed to the N=N stretching [37]. The bands of 1,306 and 1,247 cm^{-1} correspond to the C-N stretching of the secondary aromatic amine as presented in two different C-N bonds links in composites. Moreover, the absorption bands at 1083cm^{-1} due to C-H of 1-4 trisubstituted aromatic rings, and the peak at frequency 920 cm^{-1} was due to PANI film that is because of N-H out-of-plane bending. The peaks at 555cm^{-1} correspond due to the C-H vibration of aromatic in plane and aromatic out-of-plane deformation, respectively[36].In (**Figure.5c**) The FT-IR spectrum, after addition of PANI on the surface of MO was change intensity of adsorption. The characteristic vibration of PANI/MO was known to be in the region 547 - 2187 cm^{-1}. The FTIR spectra of PANI Shows the vibration around 507 cm-1 , 592 cm^{-1} , 798 cm^{-1} , 1138 cm^{-1} , 1244 cm^{-1} , 1302 cm^{-1} , 1471 cm^{-1} and 1556 cm^{-1}. The band at 507 and 592 cm^{-1} was due to stretching out of the plane, 798 cm^{-1} was C-H vibration of Para coupling benzenoid ring. The peak at 1138cm^{-1} was corresponds to C-O-C stretching of excess oxidant, 1244cm^{-1} C-N stretching of benzenoid ring, 1302cm^{-1} C-N bonds of aromatic amines, 1471cm^{-1} C=C stretching mode of vibration benzenoid and1556cm^{-1} C=N quinoid stretching mode of vibration. The peaks at 1729 cm^{-1} attributed to the C=O stretching of acetyl group. The peaks of PANI-coated MO nan-composites were slightly shifted due to the interactions between PANI and MO. The bands of C=C stretching vibrations in PANI shifted to higher wavenumber

in nan-composites demonstrating the π-π* interaction and formation of hydrogen bonding between MO and PANI. All bands in nan-composites were slightly shift, which indicate that there was strong interaction between PANI and MO.

4.4 UV-Visible Spectroscopy

Ultra violet and visible spectra were record from the synthesized in **Figure.6a) MO, b) PANI, and c) PANI/**MO using UV/Vis Spectrophotometer. In (**Figure.6a**) there was one absorption spectra of MO due to π-π* transition from valance band to conduction band at 310nm. In (**Figure. 6b**) there was one adsorption peak pure PANI shows at 313nm due to π-π* transition associated with in the benzene rings of the PANI. In (**Figure. 6c**) PANI/MO two absorption bands at ~ 308nm and ~695nm were the same as in PANI, but the peaks were slightly shifted, the first peak at 308nm, due to π-π* band transition. The second adsorption peaks at 695nm due to the molecular exaction from the highest occupied molecular orbital (HOMO) of the benzenoid rings to the lowest unoccupied molecular orbital (LUMO) quinoid rings. The red of PANI and black of MO in (**Figure.6**) shift of the inclusion transition to higher wavelength may be due to the successful interaction of MO nanoparticles within the PANI Chain. This shift might be due to the electron transition of the PANI and MO to from PANI/MO nano-composites.

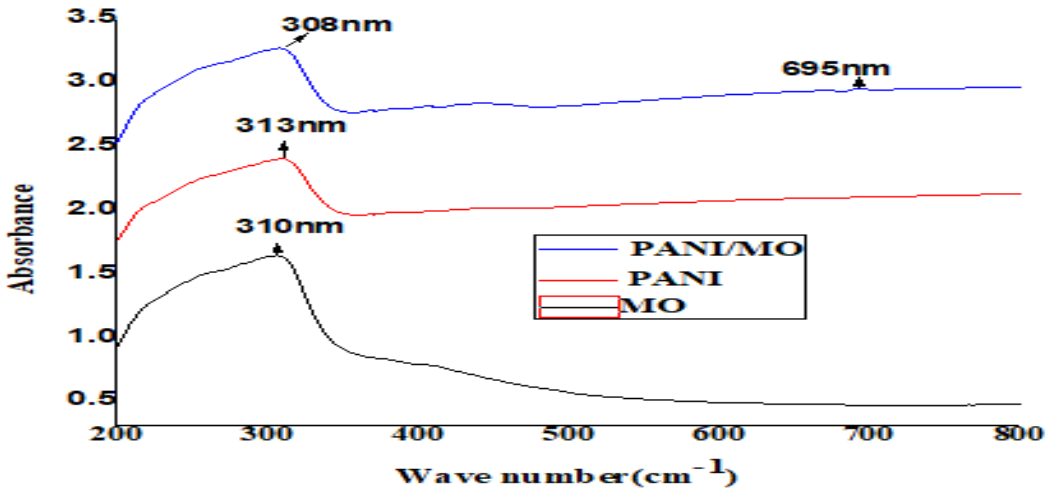

Figure. 6 UV-Vis spectra a) MO, b) PANI, and PANI/MO.

Considering the Tauc's relation in Equation (1) above, the band gap of the thin films were obtained by plotting graphs of $\alpha h\nu^{1/2}$ versus hν and extrapolating the straight portion of the graph on hυ axis at αhυ= 0. The band gap has been calculated by absorbance co-efficient data as a function wave length using Tauc relation[38]

$(\alpha h\vartheta)=\beta[h\vartheta - Eg]^{n}$……1

where α is the absorbance coefficient hϑ is the photon energy, B is the band gap tailing parameter, Eg is a characteristics energy which is termed as optical band gap and n is the transition probability index with discrete value like 1/2, 3/2, 2 or more depending on transition of direct or indirect or forbidden band gap. The absorption coefficient (α) at corresponding wavelength was calculated by using Beer Lambert's relation[38].

$$\alpha = \frac{2.303\ A}{l} \ldots\ldots\ldots\ldots\ldots\ldots\ldots\ldots\ldots\ldots\ldots\ldots\ldots\ldots\ldots\ldots\ldots 2$$

Where l is the path length and A is the absorbance

The plot (αhϑ) 1/2 vis hϑ was linear function existence of indirect allowed in transition in MO PANI, and PANI/MO. Extrapolation of linear dependence of the relation to yield corresponding band gap

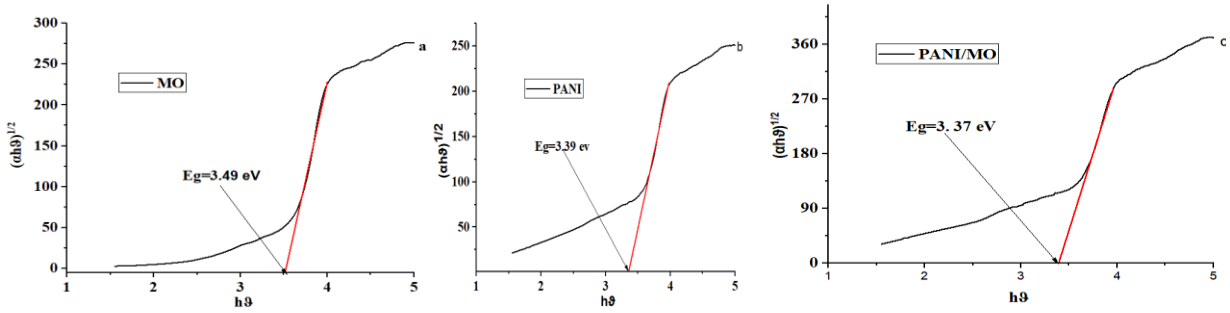

Figure. 7 Linear plot (αhϑ) 1/2 vis hϑ UV-visible band gap determination of the a) MO, b) PANI, and c) PANI/MO.

The values of the optical band gap obtained in (**Figure.7**) a) MO, b) PANI, and c) PANI/MO was calculated 3.49, 3.39 and 3.37 eV respectively. The values of optical band gap were decrease from MO to PANI/MO after deposited PANI on surface of MO with dopant APS acids implying an increase in conductivity. The reduction optical band gap due to the dimensions of resulting ions which play an important role in the process of diffusion, it was known that acids are compounds that dissociate in water only to give positive hydrogen ions and negative ions of the acid residue, the disorder of the system, and surface modifications between PANI with MO.

4.5 X-ray Diffraction (XRD) Analysis

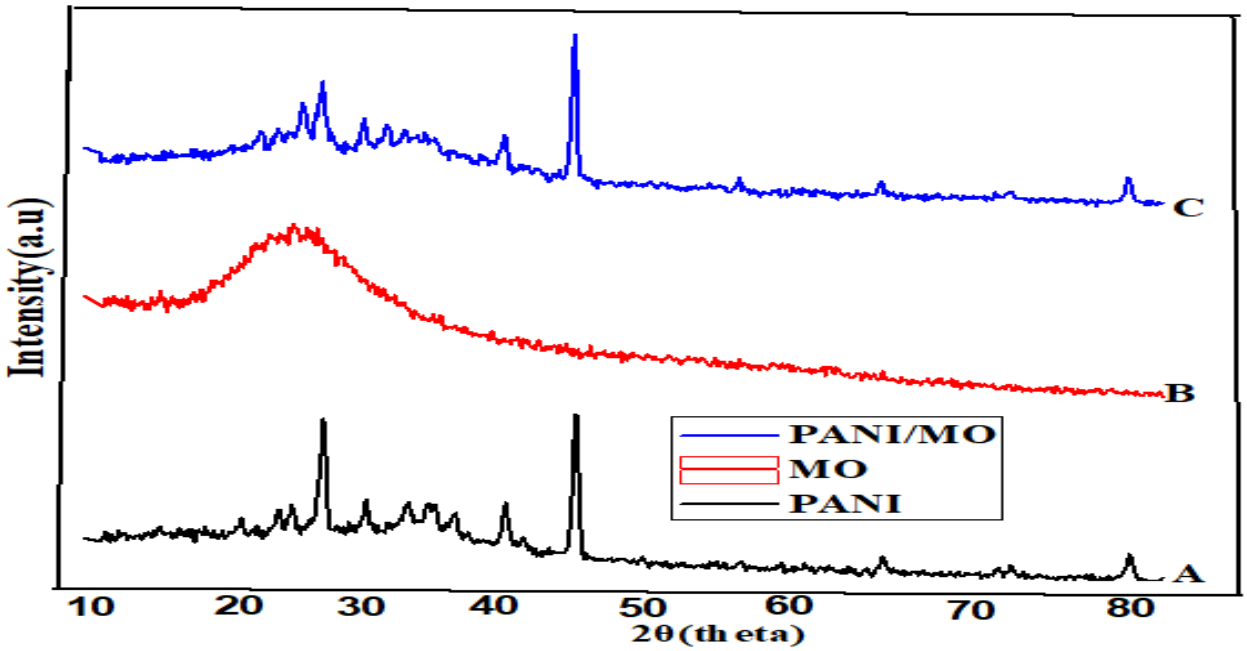

Figure.8 X-ray diffractograms of A) PANI, B) MO, C) PANI/MO.

Figure.8 A) X-ray diffraction confirms the formation of PANI, there are maximum characteristic peaks around 2θ =13.24° presented in the XRD pattern of the PANI. The crystallinity of polyaniline polycrystalline may be due to the amine and imine groups in the structure of doped PANI, which can form stronger intermolecular and intramolecular hydrogen bonds. **Figure.8 B**) shows the X-ray diffraction patterns of amorphous M. olifera seeds. Due to the high amount of proteins present in the composition of the material, around 69% by weight the X-ray pattern shows a poorly resolved peak that indicates a predominance of amorphous material. It is possible to separate a broad peak at 2θ=7.59°. The presence of this peak is probably associated with diffraction of the constituent protein surrounding the other components that have a more amorphous nature. According to Araújo et al. 2013 and Maria et al, the amorphous nature of the adsorbent suggests that the adsorbate can more easily penetrate the surface of the adsorbent, thus favoring the adsorption process[39]. **Figure.8 C**) shows the XRD patterns changes in the crystallinity of MO, upon addition of PANI Polycrystalline nature. In the XRD pattern of PANI/MO blends diffraction peaks at 2θ =7.96° correspond to the PANI emeraldine salt. The maximum peak at this angle was due to characteristic of an interlayer repeat distance of alkyl tails of counter ions that function as spacers between parallel planes of stacked PANI backbones

on MO. While the intensity of the peak at 2θ = 13.24 ° increased with PANI loading in the blend samples, the intensities of all of the other peaks decreases, signifying a lowering crystallinity upon blending with PANI. The strong intensities of the peaks indicate short-range order of the counter-ions along the polymer chain of the PANI/MO. PANI/MO was polycrystalline in nature as the patterns show sharp peaks, because of the presence of benzenoid and quinonoid group in the PANI/MO. The crystal size were calculated by Bragg's Law and Debye Scherer equation.

$$\mathbf{D=\frac{k\lambda}{\beta cos\theta}} \ldots\ldots\ldots\ldots\ldots\ldots\ldots\ldots\ldots\ldots\ldots\ldots\ldots\ldots\ldots\ldots\ldots\ldots\ldots\ldots\ldots \mathbf{1}$$

Where k= Bragg's constant (0.9) and β is the full width half maximum (FWHM) $^{1/2}$.

Table. 6 Average particle size of MO, PANI and PANI/MO sample.

Sample	2ɵ	ɵ	ɵ (radian)	Cos(ɵ)	FWHM	β(FWHM$^{1/2}$	D(nm)
MO	7.59	3.79	0.066	0.998	17.87	4.23	3.28
PANI	13.24	6.62	0.115	0.993	31.18	5.58	2.49
PANI/MO	7.96	3.98	0.069	0.998	18.74	4.34	3.20

4.6 Scanning Electron Microscopy (SEM) Analysis

The SEM micrograph of **Figure.9** a) MO, b) PANI, c) PANI/MO shows that the surface remained uniform throughout the process except a few lining structures adsorption.

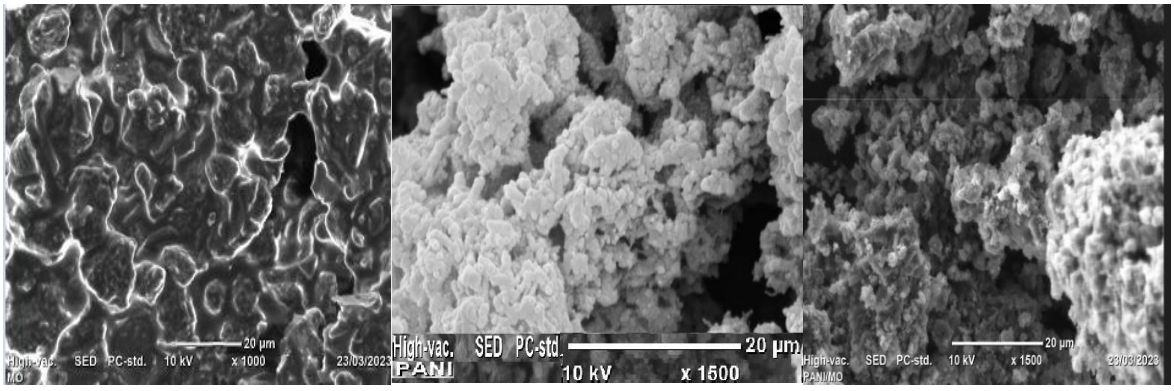

Figure. 9 Scanning electron micrograph of a) MO, b) PANI, c) PANI/MO.

Figure.9 a) Moringa olifera seeds have heterogeneous morphological characteristics, with high asymmetric porosity; it was a fibrous material, rich in cellulose and lignin. Due to the its heterogeneous surface, the good adsorption capacity of this material was attributed to the pores of the adsorbent surface; these available spaces facilitate the adsorptive process, as they provide a high internal surface of the material [40]. It is also possible to conclude, from the chemical

characteristics of Moringa olifera seeds, that chemisorption phenomenon (ionic adsorption) can occur, due to the protein groups present in the adsorbent, and morphology of this material shows a heterogeneous and relatively porous matrix. This structure facilitates the processes of ion adsorption, due to the interstices and, more importantly, to the presence of the protein component of the seed. Thus, based on these characteristics, it could conclude that this MO has an adequate morphological profile for retaining polyaniline. **Figure.9 b**) PANI was porous in nature, which shows that the material was in good shape as a porous and can be further processed for needful applications. PANI deposition was visually noticeable as the white surface globular structure. **Figure.9 c**) Aggregate observed among PANI coated MO dependently. Polyaniline deposition has shown considerable variations on the surface morphology of MO. At a glance of naked eye, in situ polymerization has completely changed dark MO to dark green suggesting that a conductive form of PANI/MO of granular structure. These morphological variations might be a result of polyaniline deposition on the surface of MO.

4.7 Electrical Conductivity Studies

The electrical conductivity of moringa olifera seed was 3.6×10^{-8} S/cm while that of pure PANI and PANI/MO were found 0.32 S/cm and 1.25×10^{-3} S/cm, respectively. The conductivity of PANI/MO was in the semiconducting level, which was clear evidence that PANI was deposited in its oxidized form. The deposition of PANI coated moringa olifera was rich in hemicellulose, lignin and other waxy substance confirmed from the FT-IR and XRD spectra. These impurities including the porous it restricted the movement of $Cu^{2+}$and Pb^{2+} in the solution.

4.8 Batch Experiments

4.8.1 Temperature Effect

Temperature is a vital parameter for both adsorption rate and equilibrium conditions as it is changing the molecular interactions and solubility [40]. The effect of temperature on the sorption of Pb^{2+} and Cu^{2+} ions was evaluated at 25, 30, 40, and 50^0c as shown in (**Figure.10**). It was observed that all processes followed the same trends. The uptake of all pollutants increased when the temperature of the system was increased. The plots recorded a sharp increase in adsorption when the temperature of the system was increased from 25 to 50^0c. This revealed that the uptake processes were endothermic in nature. The results indicated that temperature increase was a positive effect on the uptake reactions. Increasing the temperature of the system supplied the

pollutants with enough kinetic energy to overcome the hindering forces such as mass transfer resistance. Therefore, this enhanced the adsorption processes.

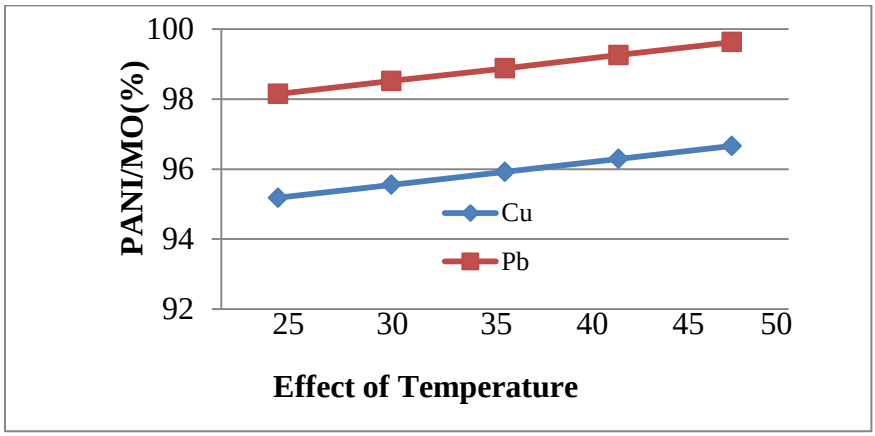

Figure. 10 Effect of Temperature on removal Percentage of PANI/MO.

4.8.2 Dosage Effect

According to the Ansari and Fahim, the much amount of Cr (IV) is adsorbe at the 0.6 g adsorbent dose. Hence this is the optimum dose for it. K. Karunakaran shows that the optimum dose is 50 mg is sufficient for the perfect removal of Fe(III) [40]. The adsorbent amount was a very effective parameter as it defines the extent of removal. In the addition to this, the removal efficiency of Cu^{2+} and Pb^{2+} ions increased from 71.17% to 99.99% with an increase of the adsorbent amount from 0.1g to 2g for 30 min of contact time. This increase in the adsorption can be related more availability of binding sites on the adsorbent surface to yield PANI/MO with Cu^{2+} and Pb^{2+}. ON the other hand Cu^{2+} and Pb^{2+} removal almost remains unchanged after (2 g) dosage of adsorbent was added since the adsorption equilibrium was reached. The maximum removal efficiency for PANI/MO composite was found at an adsorbent dosage of 2g of the composite at 25°C and for 30min of contact time in the adsorption batch experiment as can be seen from (**Figure.11)**.

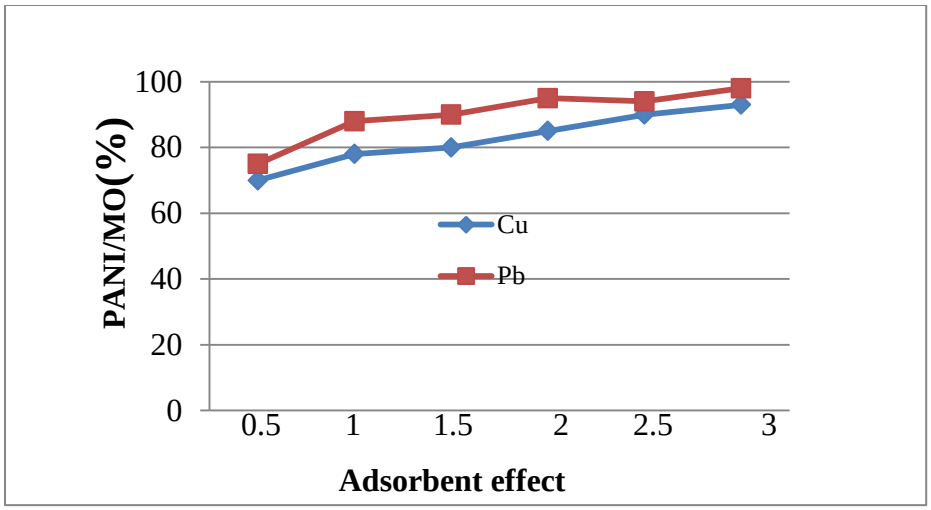

Figure. 11 Effect of adsorbent on removal Percentage of PANI/MO.

4.8.3 The effect of contact time

According to Hsu Fu-Lan et al, studied the contact time of removal of these heavy metal ions, Dl (Dendrocalamus latiflorus) adsorbed more Cd (II) and Pb (II) than Ni (II) and Cu (II) [40]. In this studies the effect of contact time was the rate of the binding possibility of Pb^{2+} and Cu^{2+} ions on the PANI/MO surface and gives the optimum contact time for removal process completion of the metal ions. **Figure.12** indicates the contact time effect on the removal efficiency of PANI/MO composite adsorbent. The removal efficiency increases with time and achieves equilibrium within 30min. The metal ion adsorption changes with time increase up to equilibrium time of 30 minutes after this point the adsorption capacity was decrease.

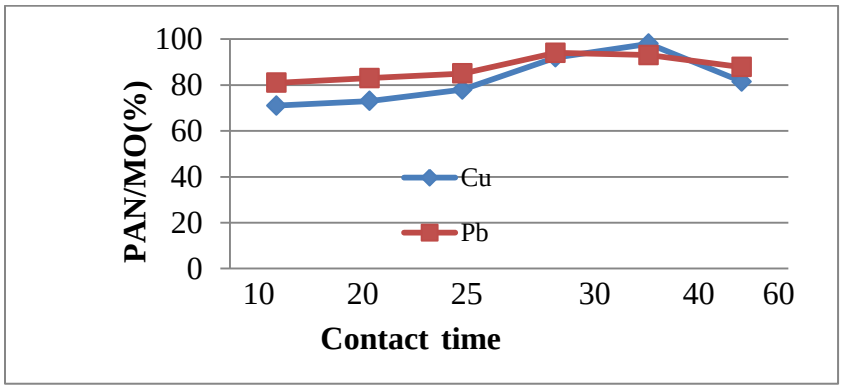

Figure. 12 Effect of Contact time on removal Percentage of PANI/MO.

4.8.4 pH Effect

According to Karunakaran K. the results indicate that the optimum dose is fixed as 50 mg due the quantity of Fe(III) uptake more, the optimum pH is fixed as 4 due to maximum removal of Fe(III) and the optimum agitation time is fixed as 30minutes thereafter removal of Fe(III) is

constant [40]. **Figure.13** indicates the PH effect on the removal efficiency of PANI/MO composite adsorbent. The percentage adsorption increases with pH to attain a maximum at 5 pH and then after it decreases with further increase in pH. The maximum removals of Cu^{2+} and Pb^{2+} at 5 pH were found to be at 99%, and 97.77%, respectively. With increase of pH from 2 to 6, the metal exists in the medium and surface protonation of adsorbent is minimum, leading to the enhancement of metal adsorption.

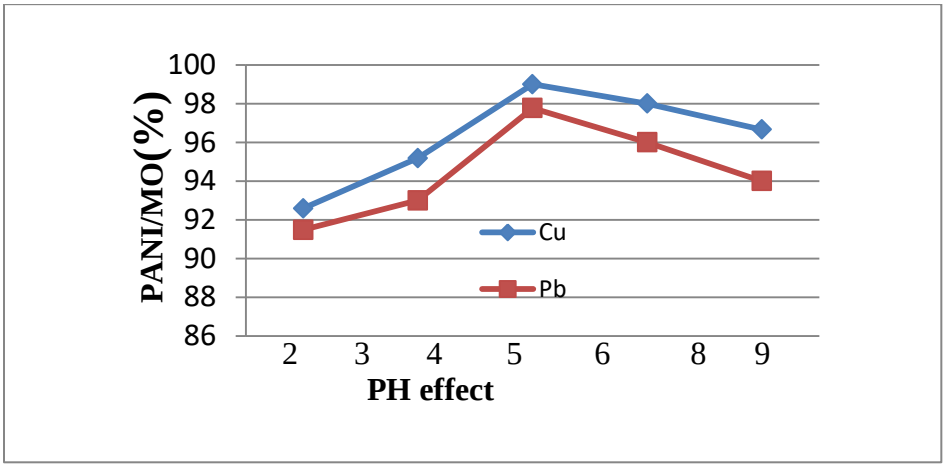

Figure. 13 Effect of pH on removal Percentage of PANI/MO.

4.8.5 Effect of Initial Concentration of Cu^{2+} and Pb^{2+}

According to Wasewar et al, Pb and Cu ion removal percentage increased when the initial ion concentration decreased[41]. The effect of initial Cu^{2+} and Pb^{2+} concentration on the Cu^{2+} and Pb^{2+} adsorption rate was studied in the rage (1-7mg/L) at pH 5, temperature 25ºC, and 30 min contact time. From the (**Figure.14**) it was observed that the percentage of removal increases with increasing in initial Cu^{2+} and Pb^{2+} concentration. For a given adsorbent dose the total number of adsorbent sites available was fixed thus adsorbing almost the equal amount of adsorbate, which resulting in a increases in the removal of adsorbate, consequent to an increase in initial Cu^{2+} and Pb^{2+} concentration. Therefore it was evident from the results that Cu^{2+} and Pb^{2+} adsorption was dependent on the initial metal concentration.

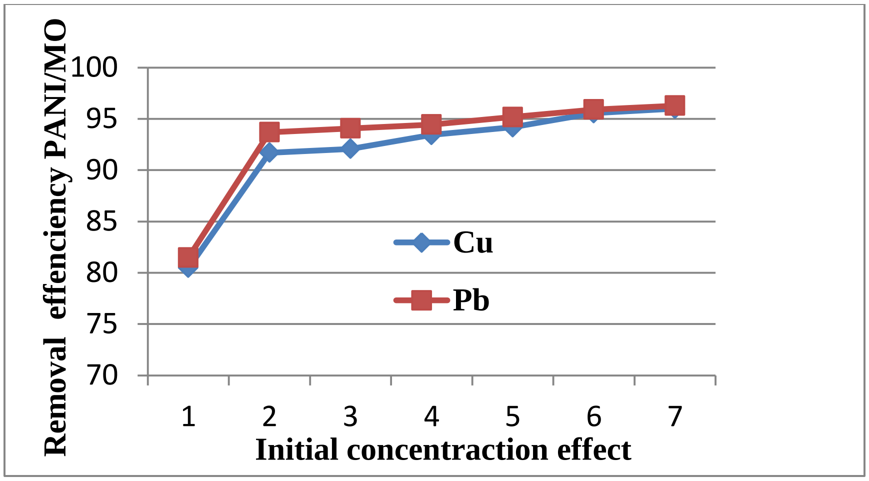

Figure. 14 Effect of Initial concentration on removal Percentage of PANI/MO.

4.9 Adsorption Study

Batch adsorption experiments was performing using a fixed mass of PANI/MO composite adsorbents by contacting with Pb^{2+}, and Cu^{2+} solution of desired concentration in 250mL stoppered bottles placed in a thermostatic shaker agitated at 250 rpm and at room temperature for desired time[42]. A series of batch experiments is conducting to study and optimize the effect of reaction time, solution pH, adsorbent dose, adsorbate initial concentration and adsorbents" particle size by agitating specific amount of adsorbent. The amount of metal ion adsorbed was calculated as [43].

C_o and C_e are Pb^{2+}, and Cu^{2+} concentration before adsorption and equilibrium concentration after adsorption, respectively, in mg/L. Removal efficiency of PANI/MO composite adsorbent will computed using Eq. 1:

Removal efficiency= $\left(\frac{C_o - C_e}{C_o}\right) x100$ ……………………………………………………… **1**

Experiments on Cu^{2+} removal from water showed that MO could remove the Cu^{2+} from the water systems up to 53.49% removal efficiency. It was report in literature that MO seeds also used to remove the Cu^{2+} from water systems and to improve the quality of drinking water. The results showed that Moringa olifera seeds were capable of absorbing the Cu^{2+} with a percentage removal of 90% [38]. In this study the removal efficiency lowest adsorption was observed (78%) for Pb^{2+} ions at pH~2.0 while the highest one (99 %) at pH~5, whereas lowest adsorption was observed (75%) for Cu^{2+} ions at pH 2.0 while the highest one (97.77%) at pH~5.

4.9.1 Langmuir Adsorption Isotherm

Langmuir model is use to describe quantitatively the formation of monolayer adsorption on the adsorbate homogeneous active sites. It also assumed that all the available adsorption sites are identical and there is no any sort of interaction between the already adsorbed chemical entities on adjacent binding sites. It can expressed in the linear form as [43].

$$\frac{Ce}{qe} = \frac{1}{qm * KL} + \frac{Ce}{qm} \ldots\ldots\ldots\ldots\ldots\ldots\ldots\ldots\ldots\ldots\ldots\ldots\ldots\ldots\ldots\ldots \mathbf{2}$$

Where C_e is the equilibrium concentration of Pb^{2+}, and Cu^{2+} in (mg/L), q_e is the amount of Pb^{2+}, and Cu^{2+} adsorbed per unit mass of adsorbent (mg/g). q_{max} and K_L are Langmuir constants associated with maximum adsorption capacity and energy of adsorption, respectively [43].

The relationship between the initial concentration of Cu^{2+} and Pb^{2+} and its percentage removal from solution was studies for all adsorbents included in the study. The initial concentrations of Cu^{2+} and Pb^{2+} studied were 2, 3, 4, and 5 mg/L at adsorbent concentration of 2g. The adsorption equilibrium data are conveniently represented by adsorption isotherms, which correspond to the relationship between the mass of the solute adsorbed per unit mass of adsorbent qe and the solute concentration for the solution at equilibrium C_e. Linear plots of C_e/q_e versus Ce (**Figure. 14 and 15**) were employed to determine the value of q_{max} (mg/g) and K_L (L/mg). In this study the value of adsorption capacity q_{max} of Cu^{2+} and Pb^{2+} was highest (10.01 and 23.01mg/g) respectively. According to McKay et al. separation factor (R_L) values between 0 and 1 indicate favorable adsorption[36]. From (**Table.7**) below the result, it was evident that the values of R_L obtained for the removal of Cu^{2+} and Pb^{2+} using PANI/MO adsorbents was (0.18 & 0.19) between 0 and 1, the adsorption process was found to be favorable and best fitted to Langmuir isotherm.

4.9.2 Freundlich Adsorption Isotherm

The emphasis of this model is to show the ratio of adsorbate adsorbed to the adsorbate concentration as a function of solution concentration. Freundlich isotherm assumes adsorption occurs at heterogeneous adsorption sites that result in multilayers formation. The amount of solute removed per unit mass of adsorbent at equilibrium is calculating using Eq.3 [43]

$$\mathbf{qe} = \frac{(\mathbf{Co} - \mathbf{Ce})\mathbf{v}}{\mathbf{m}} \ldots\ldots\ldots\ldots\ldots\ldots\ldots\ldots\ldots\ldots\ldots\ldots\ldots. \mathbf{3}$$

Where q_e is the equilibrium amount of adsorbate adsorbed per unit mass of adsorbent (mg/g), V is volume of the aqueous phase (L), and m is the amount of adsorbent used (g) [43].

$$\mathbf{logqe = log\,KF + (1/n)\,logCe} \ldots\ldots\ldots\ldots\ldots\ldots \mathbf{4}$$

Where K_F (mg g^{-1}) is the Freundlich constant and 'n' the freundlich exponent A linear graph obtained by plotting $\log^{qe}$ against $\log^{Ce}$ was determined K_F and n from intercept and slope respectively. The parameter (1/n) is related to adsorbent heterogeneity. Smaller value of (1/n) < 1 indicates more heterogeneous adsorbent sites and close to 1 indicates more homogenous binding sites [43].

The equilibrium data also fitted to Freundlich equation (Eq. (4)), a fairly satisfactory empirical isotherm can be used for non-ideal adsorption. According to Bhatt, and A. S. Sakaria, if a value of n= 1, the adsorption is linear, for $n_<$ 1, the adsorption is chemisorption, and for n > 1 the adsorption is a favorable physical adsorption. Thus, analyzing the n values > 1 for adsorption of Cu^{2+} and Pb^{2+} onto PANI/MO was much favored the physical adsorption. The adsorption capacity Kf was highest for clarified sludge followed by PANI/MO.

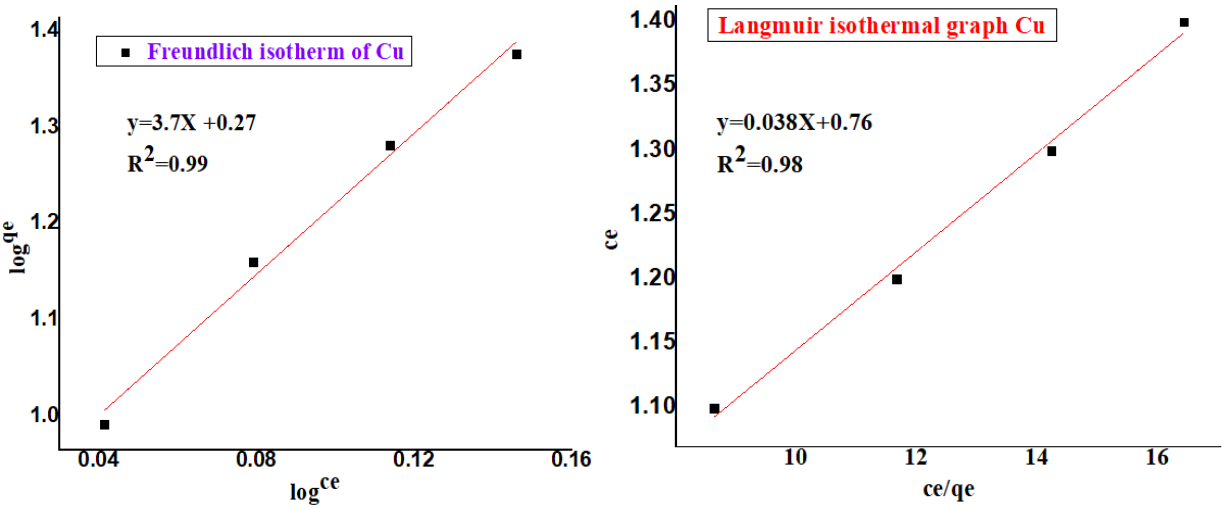

Figure 15 Langmuir and Freundlich isotherm for the adsorption of Cu^{2+} on PANI/MO.

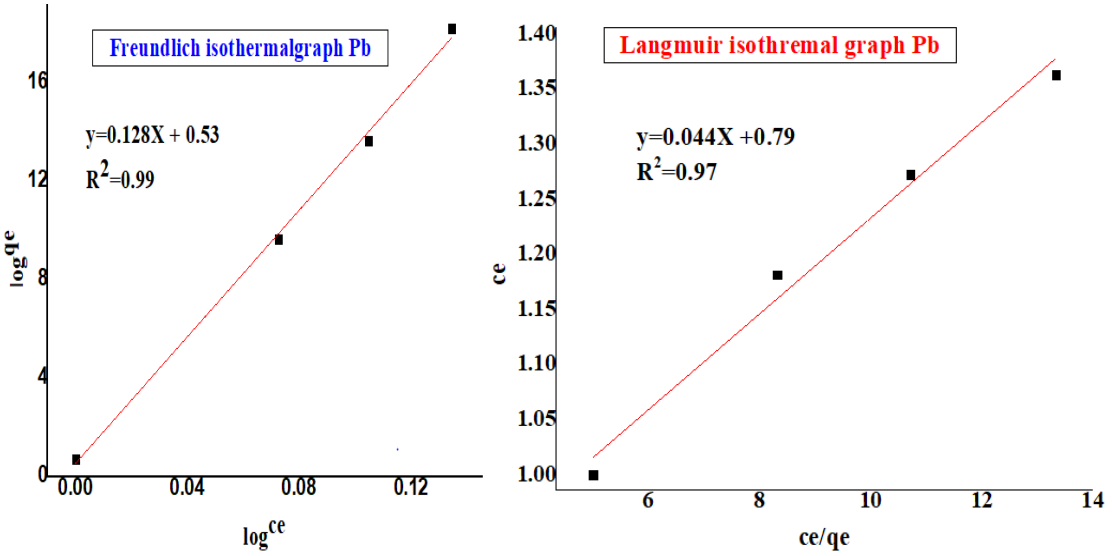

Figure. 16 Langmuir and Freundlich isotherm for the adsorption of Pb^{2+} on PANI/MO

Table. 7 Parameters for the Langmuir and Freundlich models of Cu^{2+} and Pb^{2+} on PANI/MO.

Adsorbent	Metal ion	Langmuir				Freundlich		
		q_{max}(mg/g)	K_L(L/mg)	R_L	R^2	K_f	1/n	R^2
PANI/MO	Cu^{2+}	10.01	1.32	0.18	0.99	6.91	0.27	0.99
	Pb^{2+}	23.01	1.25	0.19	0.97	1.73	0.008	0.98

Langmuir and Freundlich adsorption isotherms for Cu^{2+} and Pb^{2+} from ground water were presented in (**Table.7**) respectively. It indicates that the experimental data fitted well to all the isotherm models. By comparing the correlation coefficients, it was observed that Langmuir, and Freundlich isotherm gives a good model for the adsorption system, which was based on monolayer sorption on to the surface restraining finite number of identical sorption sites.

4.10 Kinetics of adsorption

Two types of simple kinetic models, Lagergren pseudo first order, and pseudo second order [43], were used to validate the experimental data and predict rate of uptake of adsorbate on the interface of adsorbent surface from variation in contact time. The linear form of Lagergren pseudo first and second order rate expressions are represented by Eq. 5 and 6, respectively.

$$\mathbf{ln(qe - qt) = lnqe - k1t} \ldots\ldots\ldots\ldots\ldots\ldots \mathbf{5}$$

$$\frac{t}{qt}=\frac{1}{qe2*K2}+\frac{1}{qe}t \ldots\ldots\ldots\ldots\ldots\ldots\ldots\ldots\ldots\ldots\ldots\ldots\ldots\ldots 6$$

where t is the adsorption time (min); K_1 (1/min) and K_2 [g/(mg min)] are the rate constants for the Lagergren pseudo first and pseudo second order models; q_t (mg/g) is adsorption amount at time, t(min).

Rate constant (K_1) and equilibrium adsorption capacity (qe) were determined using slope and intercept of the plot of $\ln(q_e-q_t)$ versus t from the linear expression of Lagergren pseudo first order model. The result of plot of ln(qe-qt) versus t (**Figure.17A**) is markedly deviated from linearity with correlation coefficient (R^2= 0.62). Rate constant (K_2) and equilibrium adsorption capacity (qe) were determined using slope and intercept of the plot of t/qt versus t from the linear expression of Lagergren pseudo second order model. The result of plot of t/q_t versus t (**Figure.17B**) is markedly deviated from linearity with correlation coefficient (R^2 = 1).

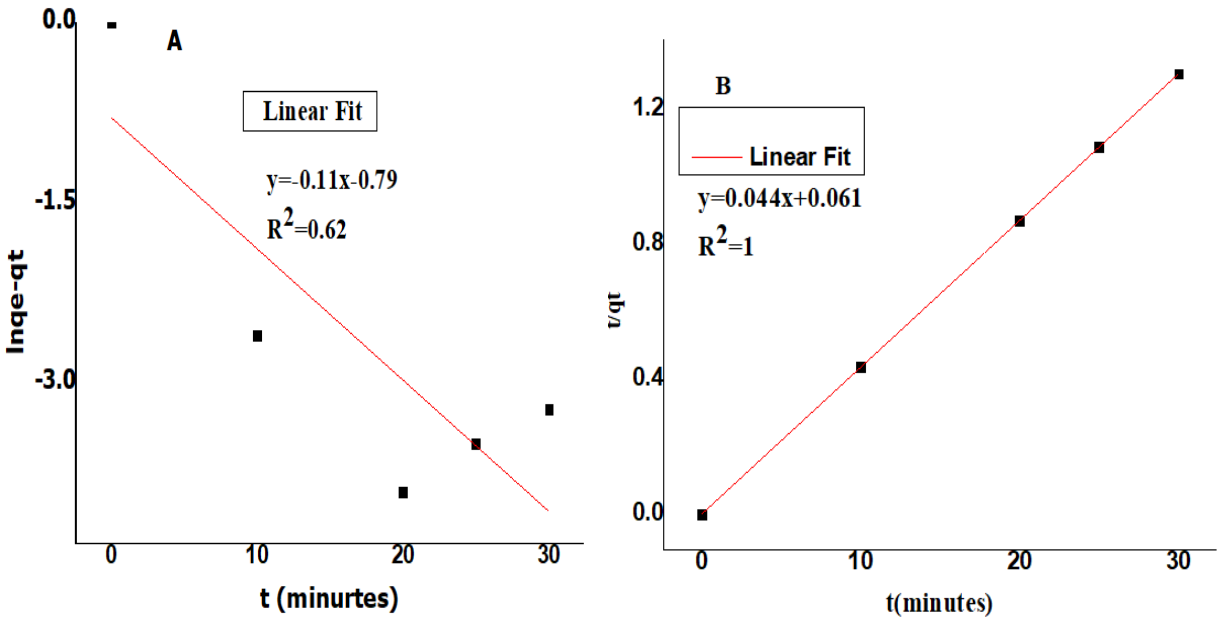

Figure. 17 Kinetic models of A) Lagergren pseudo first order B) pseudo second order adsorption of Pb^{2+}.

These findings further proved kinetic data of Pb (II) adsorption did not fit well to Lagergren pseudo first order. For this reason, experimental data was further treated using pseudo second order kinetics. The results of kinetic fitting parameter were present in (**Table.8**). The experimental equilibrium adsorption capacity (qe, exp= 23.01 mg/g) is comparably in good agreement with the theoretically computed adsorption capacity (qe, cal= 16.39 mg/g). These

findings suggest validity of pseudo second order model and physico-sorption is the rate-limiting step in Pb^{2+} adsorption process.

Rate constant (K_1) and equilibrium adsorption capacity (qe) were determined using slope and intercept of the plot of $\ln(q_e-q_t)$ versus t from the linear expression of Lagergren pseudo first order model. The result of plot of t/qt versus t (**Figure. 18 A**) is markedly deviated from linearity with correlation coefficient (R^2= 0.49). Rate constant (K_2) and equilibrium adsorption capacity (qe) were determined using slope and intercept of the plot of t/qt versus t from the linear expression of Lagergren pseudo second order model. The result of plot of t/qt versus t (**Figure. 18 B**) is markedly deviated from linearity with correlation coefficient (R^2= 0.99).

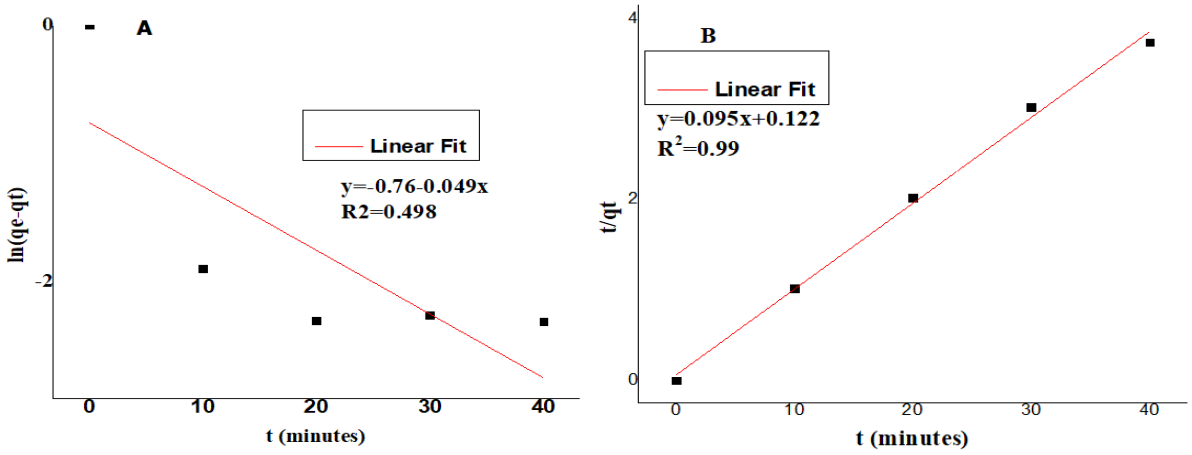

Figure. 18 Kinetic models of A) Lagergren pseudo first order B) pseudo second order adsorption of Cu^{2+}.

These findings further proved kinetic data of Cu(II) adsorption did not fit well to Lagergren pseudo first order. For this reason, experimental data was further treated using pseudo second order kinetics. Rate constant (K_2) and equilibrium adsorption capacity (qe) were calculated from the intercept and slope of plot of t/qt against t using the linear form of pseudo second order. The results of kinetic fitting parameters are presented in (**Table. 8**). The experimental equilibrium adsorption capacity (qe, exp= 10.01mg/g) is comparably in good agreement with the theoretically computed adsorption capacity (qe, cal= 8.19 mg/g). These findings suggest validity of pseudo second order model and physico-sorption is the rate-limiting step in Cu^{2+} adsorption process.

Table. 8 The pseudo first and pseudo second order kinetic parameters of Pb^{2+} and Cu^{2+} adsorption on to PANI/MO composite at 25^0C.

	Co, mg/L	Lagergren pseudo first order			qe, exp mg/g	Pseudo second order		
		R^2	qe, cal(mg/g)	K_1		R^2	qe, cal(mg/g)	K_2
Cu	5	0.49	0.47	0.049	10.01	0.99	8.19	0.095
Pb	5	0.62	0.45	0.11	23.01	1	16.39	0.044

4.10 Antimicrobial studies

To explore the antimicrobial activities of PANI/MO and agar well diffusion method (**Figure.19**) was adopt. It was interesting to note that as the concentrations of PANI/MO are increased from 0.2, 0.5 and 4.5g/mL, the zone of inhibitions increased from 6 to 15 mm for Bacillus Subtillis and 4mm to 15mm for staphylococcus aureus.

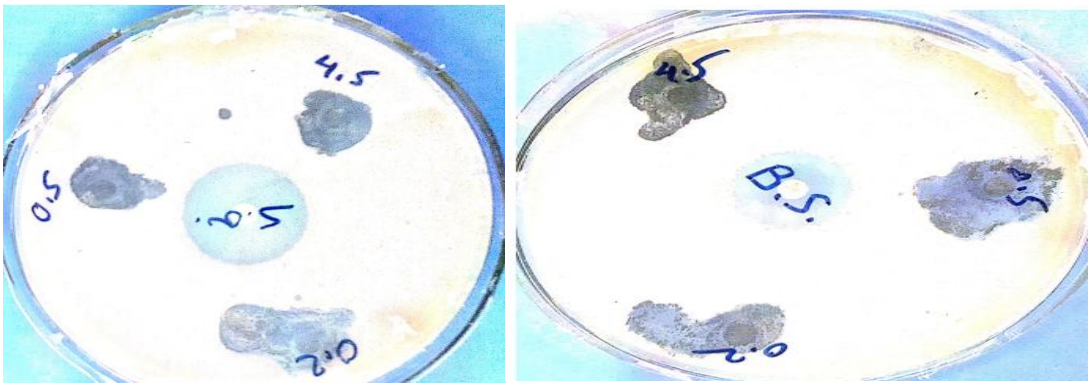

Figure. 19 Photographic images of zones of inhibition at various concentrations of PANI/MO on Staphylococcus sps and Bacillus Subtillis.

Table. 9 The concentration PANI/MO against Bacillus Subtillis and Staphylococcus aureus diameter.

Microorganism	PANI/MO		
	0.2M (0.5g)	0. 5M(0. 5g)	4. 5M (0. 5g)
Bacillus Subtillis	10mm	15mm	6mm
Staphylococcus	5mm	15mm	4mm

From (**Table.9**) it was evident that PANI/MO composite are effective against Bacillus Subtillis and Staphylococcus sps. According to Perez et al, the antibacterial effects were assessed from the diameter of zone of inhibition and minimum inhibitory concentration values. PANI and MO was found to contain antibacterial activity due to various factors such as surface hydrophobicity, length of the polymer chain, low molecular weight, electrostatic adsorption between the PANI and bacteria, direct contact between material and bacterial cells and the presence of amino groups[44]. Our present study shows that PANI/MO composite exhibited antibacterial activity against the bacterial species tested. Bacillus Subtillis was inhibited strongly (6–15 mm) by PANI/MO composite at three concentration 0.2, 0.5,4.5g/ml while PANI/MO showed only a best anti-bacteria (15 mm) at the maximum concentration tested (0.5 g/ml). Staphylococcus aureus was inhibited strongly (6–15 mm) by PANI/MO composite at three concentrations 0.2, 0.5,4.5g/ml while PANI/MO showed a best anti-bacteria (15mm) at the maximum concentration tested (0.5 g/ml).

CHAPTER FIVE: CONCLUSION AND RECOMMENDATION

5.1 CONCLUSION

PANI was successfully coat with MO using ammonium per sulfate as oxidant and dopant via in situ polymerization route. These PANI/MO composites exhibited appreciable adsorption performance towards Cu^{2+} and Pb^{2+} ion from wastewater. The results showed that PANI/MO adsorption proved to be a very effective adsorbent in the removal of Cu^{2+} and Pb^{2+} ions from ground water. Pearson correlation coefficient was used to examine the relationship between the various physico-chemical parameters four wastewater samples from all the sample sites. Therefore, Pearson correlation coefficient determined physic-chemical parameter there was strong and moderate correlation between all parameter while weak correlation turbidity another parameter. In addition to this investigation was carries out to study the suitability of a novel indigenous adsorbent PANI/MO for the removal of Cu^{2+} and Pb^{2+} from the wastewater. The influence of process parameters such as pH, adsorbent dosage, temperature, contact time, and initial metal ion concentration were at depend on removal efficiencies PANI/MO removal Cu^{2+} and Pb^{2+} from wastewater. The maximum pH of solution for Cu^{2+} and Pb^{2+} removal were found at PH ~5. MO, PANI, PANI/MO were characterized using UV-Vis spectroscopy to investigate the variations in the optical properties. The decrease in the optical band gap was due to reduction in the disorder of the system, and surface modifications of the PANI coated on MO. The adsorption data were fitted to Freundlich isotherms model was found to be the best model for both Cu^{2+} and Pb^{2+} with R^2 values (0.98 & 0.99), and 1/n value obtained from Freundlich isotherm is 0.27 & 0.008 which lies in the favorable range $0 < 1/n < 1$ respectively. Adsorption of Cu^{2+} and Pb^{2+} show that adsorption on PANI/MO was favorable. Maximum adsorption capacity of Cu^{2+} and Pb^{2+} ions wastewater on PANI/MO was 10.01mg/g & 23.01mg/g with separation factor (R_L) was between 0 to 1 which favorable to Langmuir adsorption. The characterization methods employed UV - Visible, SEM, FTIR, and XRD studies confirmed the expected structure of polymer as reported in the literature. Conductivity of PANI/MO has been measured. It is observed that there was an increase in ac conductivity for the PANI/MO sample at higher frequencies. It was evident that a PANI/MO was effective against Bacillus Subtillis and Staphylococcus aureus.

5.2 Recommendation

The following are recommended for all responsible authorities:

1. Awareness creation to the community of the study site could help them to manage some water contaminants.
2. Further studies based have to be conducted to know the source of common pollutants of the water source and to suggest possible scientific solution for the community of the study site
3. The concerned government, SNNP Water and Energy Bureau, Non-Governmental Organizations as well as the surrounding communities should discuss together for the improvement of the water quality of the study site.
4. I was recommended to use PANI/MO rather than other chemicals treatment wastewater.

6 Reference

[1] N. B. Singh, S. Rai, and S. Agarwal, “Nanoscience & Technology : Open Access Polymer Nanocomposites and Cr (VI) Removal from Water,” 2014.

[2] A. Gupta, V. Sharma, K. Sharma, V. Kumar, S. Choudhary, and P. K. Mishra, “A Review of Adsorbents for Heavy Metal Decontamination : Growing Approach to Wastewater Treatment,” pp. 1–45, 2021.

[3] L. S. Thakur and M. Parmar, “Synthetic Waste Water by Tea Waste Adsorbent,” vol. 2, no. 6, pp. 6–19, 2013.

[4] U. Chadha, S. Kumaran, Y. Sun, K. Zhu, A. Resistance, and Y. Guo, “Review paper on removal of heavy metal ions from industrial waste water effluent,” doi: 10.1088/1757-899X/1168/1/012027.

[5] H. Search, C. Journals, A. Contact, M. Iopscience, I. O. P. Conf, and I. P. Address, “Adsorption Study on Moringa Oleifera Seeds and Musa Cavendish as Natural Water Purification Agents for Removal of Lead , Nickel and Cadmium from Drinking Water,” vol. 012044, doi: 10.1088/1757-899X/136/1/012044.

[6] M. Abatal, M. T. Olguin, I. Anastopoulos, and D. A. Giannakoudakis, “Comparison of Heavy Metals Removal from Aqueous Solution by Moringa oleifera Leaves and Seeds,” 2021.

[7] V. Jadhav *et al.*, “Review Article Role of Moringa oleifera on Green Synthesis of Metal / Metal Oxide Nanomaterials,” vol. 2022, 2022.

[8] L. Eliez, C. Chatepa, and E. C. Mbewe, “Proximate , physical and chemical composition of leaves and seeds of Moringa (Moringa oleifera) from Central Malawi : A potential for increasing animal food supply in the 21 st century,” vol. 13, no. 51, pp. 2872–2880, 2018, doi: 10.5897/AJAR2018.13535.

[9] H. Hajjaoui, A. Soufi, W. Boumya, M. Abdennouri, and N. Barka, “Polyaniline / Nanomaterial Composites for the Removal of Heavy Metals by Adsorption : A Review,” 2021.

[10] A. Panel and S. In, “Polyaniline-Based Nanocomposites for Environmental Remediation Trace Metals in the Environment,” 2019, doi: 10.5772/intechopen.82384.

[11] M. Y. and Z. A. zelalem Ayana, “No Title,” 2020.

[12] A. Deda, M. Alushllari, and S. Mico, “Measurement of heavy metal concentrations in groundwater Measurement of Heavy Metal Concentrations in Groundwater,” vol. 100001, no. June 2019, pp. 3–7, 2020.

[13] P. Li, “34,203,” no. November, 2016, doi: 10.1068/a37327.Pavlovskaya.

[14] O. K. Musa and K. State, “Heavy metal concentration in groundwater around Obajana and its environs Heavy Metal Concentration in Groundwater around Obajana and Its Environs , Kogi State , North Central Nigeria,” no. January 2013, 2018.

[15] N. A. Elessawy, M. H. Gouda, M. Elnouby, S. M. Ali, and M. Salerno, “Sustainable Microbial and Heavy Metal Reduction in Water Purification Systems Based on PVA / IC Nanofiber Membrane Doped with PANI / GO,” 2022.

[16] A. Maity, T. Mahlangu, I. Arunachellan, V. Satya, N. Sypu, and L. Skosana, *Nanostructured Materials for the Removal of Inorganic Pollutants from Water and Subsequent Applications*, no. 2732. 2020.

[17] S. M. Siddeeg, M. A. Tahoon, N. S. Alsaiari, and M. Shabbir, “The Application of Functionalized Nanomaterials as an Effective Adsorbent for the Removal of Heavy Metals from Wastewater : A Review Application of Functionalized Nanomaterials as Effective

Adsorbents for the Removal of Heavy Metals from Wastewater : A Re," no. October, 2020, doi: 10.2174/1573411016999200719231712.
[18] S. F. M. Noor, N. Ahmad, M. A. Khattak, A. Mukhtar, S. Badshah, and R. U. Khan, "Removal of Heavy Metal from Wastewater : A Review of Current Treatment Processes," vol. 1, no. 1, pp. 1–9, 2019.
[19] H. Tsegaye, "COLLEGE OF NATURAL AND COMPUTATIONAL SCIENCES," no. February, 2020.
[20] K. Jiraungkoorskul and W. Jiraungkoorskul, "Moringa oleifera : A new challenge reducing heavy metal toxicity : A review," vol. 50, no. 3, pp. 199–205, 2016, doi: 10.18805/ijare.v0iOF.9361.
[21] S. O. Apori, K. Atiah, E. Hanyabui, and J. Byalebeka, "MORINGA OLEIFERA SEEDS AS A LOW-COST BIOSORBENT FOR REMOVING HEAVY METALS FROM WASTEWATER," vol. 2, no. May, 2020, doi: 10.7251/STED2002045O.
[22] K. Ravikumar and J. Udayakumar, "Moringa oleifera seed composite a novel material for hazardous heavy metals (Cd , Cr and Pb) removal from aqueous systems," vol. 11, no. 1, pp. 123–138, 2020.
[23] O. A. Abiodun and J. A. Adegbite, "Chemical and Physicochemical Properties of Moringa Flours and Oil," vol. 12, no. 5, 2012.
[24] P. C. Maity, "Polyaniline : Synthesis and Natural Nanocomposites."
[25] T. C. Maponya, M. J. Hato, and T. R. Somo, "We are IntechOpen , the world ' s leading publisher of Open Access books Built by scientists , for scientists TOP 1 % Polyaniline-Based Nanocomposites for Environmental Remediation."
[26] H. Yakişik, "Synthesis of Polyaniline / Biochar Composite Material and Modeling with Nonlinear Model for Removal of Copper (II) Heavy Metal Ions," vol. 8, no. 1, pp. 289–302, 2021.
[27] P. Ogre, S. V Ganachari, and J. S. Yaradoddi, "Synthesis and characterization polyaniline nano fibres studies of," vol. 3, no. 3, pp. 178–180, 2018, doi: 10.5185/amp.2018/015.
[28] N. Ariffin *et al.*, "Review on Adsorption of Heavy Metal in Wastewater by Using Geopolymer," *MATEC Web Conf.*, vol. 97, pp. 1–8, 2017.
[29] E. N. Ali and H. T. Seng, "Heavy Metals (Fe , Cu , and Cr) Removal from Wastewater by Moringa Oleifera Press Cake," vol. 02008, pp. 1–5, 2018.
[30] M. A. Tanko, B. Y. Sanda, and M. H. Bichi, "Application of Moringa Oleifera Seed Extract (Mose) in the Removal of Heavy Metals from Tannery Wastewater," vol. 17, no. 2, pp. 70–78, 2020.
[31] T. T. Gebretsadik, L. Wangatia, and E. Alemayehu, "Effect of Surface Modification of Sisal Fibers on Water Absorption and Mechanical Properties of Polyaniline Composite," no. June, 2017, doi: 10.1002/pc.24462.
[32] E. Yulianti *et al.*, "CHARACTERIZATION AND EFFECTIVENESS OF MORINGA OLEIFERA SEEDS EXTRACT AS A," vol. 12, no. 2, pp. 57–64, 2020.
[33] I. Of, D. In, I. Oxides, and N. For, "Characterization and use of Moringa oleifera seeds as biosorbent for removing metal ions from aqueous effluents," no. September 2014, 2010, doi: 10.2166/wst.2010.419.
[34] A. Mostafaei and A. Zolriasatein, "Progress in Natural Science : Materials International Synthesis and characterization of conducting polyaniline nanocomposites containing ZnO nanorods," *Prog. Nat. Sci. Mater. Int.*, vol. 22, no. 4, pp. 273–280, 2012, doi: 10.1016/j.pnsc.2012.07.002.

[35] M. Ibrahim and E. Koglin, “Spectroscopic Study of Polyaniline Emeraldine Base : Modelling Approach,” no. May, 2014.
[36] S. K. Singh, A. K. Verma, and R. K. Shukla, “Original Research Article Synthesis and optical studies of pure polyaniline film,” vol. 3, no. 7, pp. 512–517, 2014.
[37] J. E. De Albuquerque, L. H. C. Mattoso, and R. M. Faria, “Study of the interconversion of polyaniline oxidation states by optical absorption spectroscopy,” vol. 146, pp. 1–10, 2004, doi: 10.1016/j.synthmet.2004.05.019.
[38] J. O. Ozuomba, “SYNTHESIS AND OPTICAL CHARACTERIZATION OF ACID-DOPED POLYANILINE THIN FILMS,” vol. 37, no. 1, pp. 135–138, 2018.
[39] V. Sridevi, S. Malathi, and C. S. Devi, “Synthesis and Characterization of Polyaniline / Gold Nanocomposites,” vol. 2011, pp. 1–6, 2011.
[40] M. Arsalan, I. Siddique, A. Awais, M. Baoji, and I. Khan, “Highly Ef fi cient PANI-WH Novel Composite for Remediation of Ni (II), Pb (II), and Cu (II) From Wastewater,” vol. 10, no. June, pp. 1–12, 2022, doi: 10.3389/fenvs.2022.895463.
[41] B. Alawa, A. Srivastava, J. K. Srivastava, and J. Palsaniya, “Novus International Journal of Engineering & Technology Adsorption of heavy metals from industrial downstream using polypyrrole as a polycomposite material,” vol. 3, no. 1, pp. 35–46, 2014.
[42] T. Brahmaiah, L. Spurthi, K. Chandrika, L. K. C. L, and S. Yashas, “Removal of Heavy Metals from Waste Water Using Low Cost Adsorbent,” vol. 3, no. 1, 2016.
[43] X. Wang, Y. Guo, L. Yang, M. Han, J. Zhao, and X. Cheng, “Journal of Environmental & Nanomaterials as Sorbents to Remove Heavy Metal Ions in Wastewater Treatment,” vol. 2, no. 7, 2012, doi: 10.4172/2161-0525.1000154.
[44] L. N. Shubha, M. Kalpana, and P. M. Rao, “Synthesis , characterization by AC conduction and antibacterial properties of polyaniline fibers,” vol. 8, no. 1, pp. 214–219, 2016.

7 APPENDIX

One-Way ANOVA						
		Sum of Squares	Df	Mean Square	F	Sig.
PH	Between Groups	.763	3	.254	1386.955	.000
	Within Groups	.001	8	.000		
	Total	.764	11			
EC	Between Groups	26686.182	3	8895.394	10610.808	.000
	Within Groups	6.707	8	.838		
	Total	26692.889	11			
TUR	Between Groups	21.563	3	7.188	13.800	.002
	Within Groups	4.167	8	.521		
	Total	25.729	11			
TSS	Between Groups	1691.729	3	563.910	458.774	.000
	Within Groups	9.833	8	1.229		
	Total	1701.563	11			
TDS	Between Groups	10638.990	3	3546.330	7954.385	.000
	Within Groups	3.567	8	.446		
	Total	10642.557	11			
TA	Between Groups	161619.000	3	53873.000	189.139	.000
	Within Groups	2278.667	8	284.833		
	Total	163897.667	11			
TH	Between Groups	274717.333	3	91572.444	434.164	.000
	Within Groups	1687.333	8	210.917		
	Total	276404.667	11			
Temp	Between Groups	.090	3	.030	1.440	.302
	Within Groups	.167	8	.021		
	Total	.257	11			
Cl	Between Groups	6148.223	3	2049.408	158.776	.000
	Within Groups	103.260	8	12.908		
	Total	6251.483	11			
Pb	Between Groups	4.242	3	1.414	10.041	.004
	Within Groups	1.127	8	.141		
	Total	5.369	11			
Cu	Between Groups	9.000	3	3.000	17.910	.001
	Within Groups	1.340	8	.167		
	Total	10.340	11			

Multiple Comparisons							
LSD'							
Dependent Variable	(I) SL	(J) SL	Mean Difference (I-J)	Std. Error	Sig.	95% Confidence Interval	
						Lower Bound	Upper Bound
pH	Gubre	WES	-.48000*	.01106	.000	-.5055	-.4545
		MT	-.40000*	.01106	.000	-.4255	-.3745
		THC	-.69667*	.01106	.000	-.7222	-.6712
	WES	Gubre	.48000*	.01106	.000	.4545	.5055
		MT	.08000*	.01106	.000	.0545	.1055
		THC	-.21667*	.01106	.000	-.2422	-.1912
	MT	Gubre	.40000*	.01106	.000	.3745	.4255
		WES	-.08000*	.01106	.000	-.1055	-.0545
		THC	-.29667*	.01106	.000	-.3222	-.2712
	THC	Gubre	.69667*	.01106	.000	.6712	.7222
		WES	.21667*	.01106	.000	.1912	.2422
		MT	.29667*	.01106	.000	.2712	.3222
EC	Gubre	WES	-112.66667*	.74759	.000	-114.3906	-110.9427
		MT	-98.90000*	.74759	.000	-100.6239	-97.1761
		THC	-112.80000*	.74759	.000	-114.5239	-111.0761
	WES	Gubre	112.66667*	.74759	.000	110.9427	114.3906
		MT	13.76667*	.74759	.000	12.0427	15.4906
		THC	-.13333	.74759	.863	-1.8573	1.5906
	MT	Gubre	98.90000*	.74759	.000	97.1761	100.6239
		WES	-13.76667*	.74759	.000	-15.4906	-12.0427
		THC	-13.90000*	.74759	.000	-15.6239	-12.1761
	THC	Gubre	112.80000*	.74759	.000	111.0761	114.5239
		WES	.13333	.74759	.863	-1.5906	1.8573
		MT	13.90000*	.74759	.000	12.1761	15.6239
TUR	Gubre	WES	2.16667*	.58926	.006	.8078	3.5255
		MT	-1.50000*	.58926	.034	-2.8588	-.1412
		THC	-.50000	.58926	.421	-1.8588	.8588
	WES	Gubre	-2.16667*	.58926	.006	-3.5255	-.8078
		MT	-3.66667*	.58926	.000	-5.0255	-2.3078
		THC	-2.66667*	.58926	.002	-4.0255	-1.3078
	MT	Gubre	1.50000*	.58926	.034	.1412	2.8588
		WES	3.66667*	.58926	.000	2.3078	5.0255
		THC	1.00000	.58926	.128	-.3588	2.3588
	THC	Gubre	.50000	.58926	.421	-.8588	1.8588
		WES	2.66667*	.58926	.002	1.3078	4.0255
		MT	-1.00000	.58926	.128	-2.3588	.3588
TSS	Gubre	WES	-9.83333*	.90523	.000	-11.9208	-7.7459
		MT	-21.00000*	.90523	.000	-23.0875	-18.9125
		THC	-31.66667*	.90523	.000	-33.7541	-29.5792
	WES	Gubre	9.83333*	.90523	.000	7.7459	11.9208
		MT	-11.16667*	.90523	.000	-13.2541	-9.0792
		THC	-21.83333*	.90523	.000	-23.9208	-19.7459
	MT	Gubre	21.00000*	.90523	.000	18.9125	23.0875
		WES	11.16667*	.90523	.000	9.0792	13.2541
		THC	-10.66667*	.90523	.000	-12.7541	-8.5792
	THC	Gubre	31.66667*	.90523	.000	29.5792	33.7541
		WES	21.83333*	.90523	.000	19.7459	23.9208
		MT	10.66667*	.90523	.000	8.5792	12.7541
TDS	Gubre	WES	-74.50000*	.54518	.000	-75.7572	-73.2428
		MT	-58.66667*	.54518	.000	-59.9239	-57.4095
		THC	-69.30000*	.54518	.000	-70.5572	-68.0428
	WES	Gubre	74.50000*	.54518	.000	73.2428	75.7572
		MT	15.83333*	.54518	.000	14.5761	17.0905
		THC	5.20000*	.54518	.000	3.9428	6.4572

	MT	Gubre	58.66667*	.54518	.000	57.4095	59.9239
		WES	-15.83333*	.54518	.000	-17.0905	-14.5761
		THC	-10.63333*	.54518	.000	-11.8905	-9.3761
	THC	Gubre	69.30000*	.54518	.000	68.0428	70.5572
		WES	-5.20000*	.54518	.000	-6.4572	-3.9428
		MT	10.63333*	.54518	.000	9.3761	11.8905
TA	Gubre	WES	-319.66667*	13.78002	.000	-351.4434	-287.8899
		MT	-219.66667*	13.78002	.000	-251.4434	-187.8899
		THC	-202.66667*	13.78002	.000	-234.4434	-170.8899
	WES	Gubre	319.66667*	13.78002	.000	287.8899	351.4434
		MT	100.00000*	13.78002	.000	68.2232	131.7768
		THC	117.00000*	13.78002	.000	85.2232	148.7768
	MT	Gubre	219.66667*	13.78002	.000	187.8899	251.4434
		WES	-100.00000*	13.78002	.000	-131.7768	-68.2232
		THC	17.00000	13.78002	.252	-14.7768	48.7768
	THC	Gubre	202.66667*	13.78002	.000	170.8899	234.4434
		WES	-117.00000*	13.78002	.000	-148.7768	-85.2232
		MT	-17.00000	13.78002	.252	-48.7768	14.7768
TH	Gubre	WES	-408.66667*	11.85796	.000	-436.0112	-381.3222
		MT	-308.66667*	11.85796	.000	-336.0112	-281.3222
		THC	-272.00000*	11.85796	.000	-299.3445	-244.6555
	WES	Gubre	408.66667*	11.85796	.000	381.3222	436.0112
		MT	100.00000*	11.85796	.000	72.6555	127.3445
		THC	136.66667*	11.85796	.000	109.3222	164.0112
	MT	Gubre	308.66667*	11.85796	.000	281.3222	336.0112
		WES	-100.00000*	11.85796	.000	-127.3445	-72.6555
		THC	36.66667*	11.85796	.015	9.3222	64.0112
	THC	Gubre	272.00000*	11.85796	.000	244.6555	299.3445
		WES	-136.66667*	11.85796	.000	-164.0112	-109.3222
		MT	-36.66667*	11.85796	.015	-64.0112	-9.3222
Temp	Gubre	WES	-.20000	.11785	.128	-.4718	.0718
		MT	.00000	.11785	1.000	-.2718	.2718
		THC	-.13333	.11785	.291	-.4051	.1384
	WES	Gubre	.20000	.11785	.128	-.0718	.4718
		MT	.20000	.11785	.128	-.0718	.4718
		THC	.06667	.11785	.587	-.2051	.3384
	MT	Gubre	.00000	.11785	1.000	-.2718	.2718
		WES	-.20000	.11785	.128	-.4718	.0718
		THC	-.13333	.11785	.291	-.4051	.1384
	THC	Gubre	.13333	.11785	.291	-.1384	.4051
		WES	-.06667	.11785	.587	-.3384	.2051
		MT	.13333	.11785	.291	-.1384	.4051
Cl	Gubre	WES	-61.10000*	2.93343	.000	-67.8645	-54.3355
		MT	-41.10000*	2.93343	.000	-47.8645	-34.3355
		THC	-46.10000*	2.93343	.000	-52.8645	-39.3355
	WES	Gubre	61.10000*	2.93343	.000	54.3355	67.8645
		MT	20.00000*	2.93343	.000	13.2355	26.7645
		THC	15.00000*	2.93343	.001	8.2355	21.7645
	MT	Gubre	41.10000*	2.93343	.000	34.3355	47.8645
		WES	-20.00000*	2.93343	.000	-26.7645	-13.2355
		THC	-5.00000	2.93343	.127	-11.7645	1.7645
	THC	Gubre	46.10000*	2.93343	.000	39.3355	52.8645
		WES	-15.00000*	2.93343	.001	-21.7645	-8.2355
		MT	5.00000	2.93343	.127	-1.7645	11.7645
Pb	Gubre	WES	-1.10000*	.30641	.007	-1.8066	-.3934
		MT	-1.10000*	.30641	.007	-1.8066	-.3934
		THC	-1.63333*	.30641	.001	-2.3399	-.9267
	WES	Gubre	1.10000*	.30641	.007	.3934	1.8066
		MT	.00000	.30641	1.000	-.7066	.7066

		THC	-.53333	.30641	.120	-1.2399	.1733
	MT	Gubre	1.10000*	.30641	.007	.3934	1.8066
		WES	.00000	.30641	1.000	-.7066	.7066
		THC	-.53333	.30641	.120	-1.2399	.1733
	THC	Gubre	1.63333*	.30641	.001	.9267	2.3399
		WES	.53333	.30641	.120	-.1733	1.2399
		MT	.53333	.30641	.120	-.1733	1.2399
Cu	Gubre	WES	-.40000	.33417	.266	-1.1706	.3706
		MT	-1.60000*	.33417	.001	-2.3706	-.8294
		THC	-2.13333*	.33417	.000	-2.9039	-1.3627
	WES	Gubre	.40000	.33417	.266	-.3706	1.1706
		MT	-1.20000*	.33417	.007	-1.9706	-.4294
		THC	-1.73333*	.33417	.001	-2.5039	-.9627
	MT	Gubre	1.60000*	.33417	.001	.8294	2.3706
		WES	1.20000*	.33417	.007	.4294	1.9706
		THC	-.53333	.33417	.149	-1.3039	.2373
	THC	Gubre	2.13333*	.33417	.000	1.3627	2.9039
		WES	1.73333*	.33417	.001	.9627	2.5039
		MT	.53333	.33417	.149	-.2373	1.3039

*. The mean difference is significant at the 0.05 level.